12-12-2022

Testing Detrital Zircon age Bias in Tectonic Provenance: Examples from Modern Alluvium in the South Island, New Zealand

Will Sparhawk Fisher
Syracuse University

Abstract

Detrital zircon (DZ) grains from 13 drainages across the South Island, New Zealand, were U-Pb dated to ascertain how accurately their ages reflect the geologic record of exposed bedrock. With the proliferation of inexpensive and easily accessible ion microprobes and laser ablation inductively coupled plasma mass spectrometers, DZ dating has become the dominant chronometer for elucidating tectonic systematics. Zircon's physical and chemical resilience makes it an ideal candidate for U-Pb geochronometry, but is also a potential source of bias. Zircon's resilience in sedimentary systems means it rarely occurs as first order detritus. N = 966 zircon grains from Modern alluvium were U-Pb dated and statistically scrutinized against sedimentary and plutonic bedrock grain-age compilations in the published literature. Cross-correlation, Likeness, Similarity, and Kolmogorov-Smirnoff tests were employed to better understand how well DZ in modern alluvium are representing the bedrock. Even with minimal analyses of populations, grain-age distributions in the modern alluvium are missing from the bedrock on the South Island, New Zealand. Thus, although DZ is a significant tool for constraining some aspects of tectonics and sedimentary provenance it needs to be interpreted cautiously in assuming a one-to-one relationship between potential bedrock source and sedimentary sink.

Testing Detrital Zircon age Bias in Tectonic Provenance: Examples from Modern Alluvium in the South Island, New Zealand

By

Will S. Fisher

B.S. in Geology, Union College, 2019

Thesis
Submitted in partial fulfillment of the requirements for the degree
of M.S. in Earth Sciences

Syracuse University
December 2022

Table of Contents

INTRODUCTION

U-Pb dating of detrital zircon ($ZrSiO_4$) is a well established technique in constraining sedimentary provenance and aiding in tectonic reconstructions (Compston and Pidgeon, 1986). The explosion of detrital zircon (DZ) analysis is driven by increased access to ion microprobes and laser ablation inductively coupled plasma mass spectrometers (ICP-MS) (Froude, *et al.*, 1983). Thousands of DZ studies have been conducted, but it is unclear how much information is being lost in sedimentary systems that have not well characterized DZ biases (e.g., O'Sullivan et al., 2016). Zircon-rich source terranes can dominate a sedimentary system, i.e., the zircon fertility problem discussed by Moecher and Samson (2006), whereas terranes dominated by metamorphic rocks are likely to be zircon poor and thus underrepresented in the DZ record (e.g. O'Sullivan *et al.*, 2016). Some of the very same properties intrinsic to making zircon a robust chronometer serve as bias for elucidating low-grade metamorphic and tectonic events. Zircon is important for understanding Earth's major magmatic events, however, it is essentially inert to regional metamorphism until amphibolite to granulite facies metamorphism (Rubatto, *et al.*, 2001; Williams, 2001). An entire cycle of crustal loading, terrane amalgamation, and subduction could occur at low to medium grade metamorphic pressures and temperatures, yet the zircon record would not reflect such events. Another possibility, is that only one tectonic subevent was a large zircon producing one, making the rest of the tectonic cycle unresolvable with traditional analysis and sampling methods (Moecher and Samson, 2006). Thus, understanding and quantifying sedimentary biases is crucial to provenance and tectonic studies that rely heavily on detrital minerals (Campbell, 2020; Rosenbaum, *et al.*, 2020).

Rapid and relatively inexpensive U-Pb geochronological techniques have revolutionized our understanding of provenance and terrane accretion, but DZ dating is not without potential sources of bias. For instance, although zircon's physical and chemical resilience is an asset, it also allows for potential bias in the sedimentary record. One of the major forms of bias is due to its incredible resistance; it rarely occurs as first-order detritus as it often survives multiple recycling events. However, there are other potential biases when relying solely on the DZ age record. (1) The generally very high formation temperatures during magma crystallization, thus causing zircon to be 'absent' in lower grade tectonic events (i.e., those that are largely metamorphic not reaching amphibolite or granulite facies metamorphism (Rubatto *et al.,* 2001). (2) a sedimentary record that is biased towards zircon-rich source terranes that erode more zircon compared to average zircon-bearing crustal regions (Moecher and Samson, 2006), (3) substantial differences in topographic elevation/erodibility of a crustal region (Mapes *et al.,* 2004, 2005), and (4) metamorphic zircons that have "grown" rims could bias a grain-age population if an analysis overlaps multiple age zones (Nemchin, *et al*., 2001). The zircon age populations within modern alluvium samples may therefore reflect variable biases derived from: differing source rock compositions, the extents of aerial exposures, source rock lithologies that are diachronously and laterally eroding differently, and how carefully the grains are analyzed.

To ascertain whether DZ is accurately representing the geologic record, a suite of detrital zircon from modern alluvium was dated from a tectonically and geochronologically well characterized part of the world: parts of the the South Island, New Zealand. Age spectra from detrital zircon across a diverse array of watersheds were statistically scrutinized and compared with exposed bedrock-Pb zircon age peaks from the South Island. A plethora of rivers drain the uplifted eroding bedrock in this area, making their alluvium an excellent target for examining detrital minerals to compare to the record from exposed bedrock. This study examines how well the detrital geochronological database compares to the known extent of radiometrically well-defined bedrock and what inferences can made from these comparisons.

BACKGROUND

1. Geologic Setting & Tectonic Framework

Zealandia, a 4.9 million km^2 region of the southwest Pacific Ocean located between ~25°-56°S and 160°E-168°W, provides a fresh framework for reexamining and investigating tectonic processes (Mortimer *et al*., 2017, Mortimer, 2004; Timm *et al*., 2010). It has an elevated bathymetry relative to surrounding oceanic crust and a thick, low-velocity silica-rich crust defining it as a continent. As a result of Late Cretaceous crustal thinning and subsequent continental rifting, today 94% of the continent is submerged (Mortimer *et al*., 2017). The only emergent parts of Zealandia are New Caledonia, New Zealand, four groups of Subantarctic islands (Antipodes, Auckland, Campbell, and Chatam Islands) (Adams *et al*., 2017, Mortimer, 2006, Timm *et al*., 2010). The submerged parts of Zealandia comprise the Boundary Trough, Chatam Rise in the East, Challenger Plateau and Lord Howe Rise in the northwest, and the Campbell Plateau (Timm et al.,2010).

Zealandia, prior to 84 Ma, formed a section of the eastern Gondwana convergent margin, subducting proto-Pacific basin plates (Mortimer, 2006). Subduction took place beneath this margin from the Paleozoic-Mesozoic until it ceased in the Early Cretaceous, subsequently followed by rifting of crust forming the Tasman Sea Basin (Mortimer *et al*., 2017). The margin underwent an abrupt change 116-100 Ma with the cessation of compressional tectonics to be replaced by an extensional regime (Schwartz *et* al., 2016). The Mesozoic convergent margin is represented today by the Torlesse-Haast schist accretionary complex and Median Batholith magmatic arc. Approximately 45 Ma, during the Early Miocene, a spreading center propagated northeastward into Zealandia, resulting in the modern northern and southern islands. Today the regional tectonics of New Zealand are dominated by two subduction centers and the Alpine Fault. To the northeast the Pacific plate is subducting along the Hikurangi Margin and to the southwest along the Fiordland Margin (Walcott, 1978). The Alpine Fault, the northward continuation of which is the Wairau Fault, separates very different lithologies and ages with at least 460 km of offset across it (Walcott, 1978).

Today, the South Island is cut along the Alpine Fault and has been dextrally offset by ~750 km since the latest Oligocene (i.e., since ~ 25 Ma) (Lamb and Mortimer, 2021; Figures 1 and 2). Uplift and exhumation accompanying formation of the Southern Alps, driven from the Late Miocene, is principally a result of transpressive strike-slip motion and convergence (Walcott, 1978). The South Island is volumetrically dominated by metasedimentary terranes accreted to Gondwanan basement rocks since the Cambrian (Adams et al., 2002). These include a diverse range of Cretaceous rocks, primarily schists, granitoids, granulites, and greywackes, that comprise most of the South Island. The pre-Late Cretaceous basement rocks are subdivided into two geological units: The Western and Eastern Provinces (Fig. 1) The Western Province comprises the Takaka and Buller terranes and was part of the early Paleozoic foreland of eastern Gondwana (Adams *et al.*, 2017, Mortimer, 2008).

The Eastern Province is dominated by a mosaic of autochthonous and allochthonous subduction and accretionary wedge-related continental foreland terranes (Adams *et al.*, 2002; 2017). Several tectonostratigraphic terranes comprise the Eastern Province: The Caples, Waipapa, Torlesse Composite, and Boghen terranes (Campbell *et al*., 2020). These terranes represent a paleo-oceanic margin, containing low-grade metasedimentary successions of an accretionary complex (Campbell, *et al*., 2020). The Central Arc terranes, located between the accretionary complex terranes and the Western Province of New Zealand, consist of: the Brook Street, Murihiku, Kaka Point Structural Belt, and Dun Mountain-Maitai terranes (Campbell *et al*., 2020). The same Central Arc terranes can be seen on New Caledonia with the Koh-Central and Téremba terranes (Campbell *et al*., 2020). The Murihiku, Kaka Structural Point, and Brook Street Terranes, are fault bounded against the Dun-Mountain Maitia Terrane, which is underlain by the Caples Terrane, (Turnbull, 2003). The Brook Street Terrane (containing mafic lavas and plutonic rocks) and the Dun Mountain-Maitai (ophiolitic complexes) represent arc-related basins (Campbell *et* al., 2020). The provenance, position, and original tectonic setting of the Eastern Province terranes is suspect and still debated today (Campbell *et* al., 2020; Mortimer, 2008). Samples in this study were collected from alluvium from rivers draining the pre-Late Cretaceous basement rocks across the Western and Eastern Provinces, however the majority of samples were collected from the Eastern Province (Fig. 1). These terranes have likely been crustally reworked multiple times and include zircons from a wide array of Gondwanan sources.

The Eastern Province terranes are suspect; because their original paleogeographical setting with respect to Zealandia is uncertain. Suspect terranes were first defined by Coney *et al* (1980). Suspect terranes have internal homogeneousness and continuous sections of stratigraphy, bounded by faults or unconformities (Coney *et al*., 1980). The amalgamation and timing of the Eastern Province terranes is unclear. These terranes can extend 1,000s of km's, be >200 km wide, and km's deep, thus they need a comparable source region, not present in Zealandia today. Adams *et al* (1998), proposes that the Eastern Province samples originated parallel to the

Carboniferous-Triassic, New England Fold-Belt of northeastern Australia. One possible explanation for their current positioning, is progressive anti-clockwise displacement with respect to the Gondwanaland margin (Adams *et al*., 1998). In the last 100-80 Ma, this could have accommodated the necessary 2,000 km at 225-20 mm/yr (Adams *et al*., 1998).

2. U/Pb GEOCHRONOLOGY AND RADIOMETRIC DATING

Isotopic geochronology is the cornerstone to understanding the temporal relationships between geologic bodies. The most used chromometer today is based on the U-Pb decay series. Secular equilibrium for this system with a parent and final stable daughter product can be simplified to:

$$N_1\lambda_1 = N_2\lambda_2 = N_3\lambda_3 = \ldots$$

Where Nx represents the moles of the parent isotope and λ_x the decay constant of that specific radioactive parent (grandparent, great-grandparent, etc) (Bourdon *et al*., 2003). The power of the U-Pb geochronological system lies in the three independent decay systems contained within, that can be implemented:

$$\textbf{(1)}\quad ({}^{206}Pb/{}^{204}Pb) = ({}^{206}Pb/{}^{204}Pb)_0 + ({}^{238}U/204)Pb)e^{\lambda 238t-1}$$

$$\textbf{(2)}\quad ({}^{207}Pb/{}^{204}Pb) = ({}^{207}Pb/{}^{204}Pb)_0 + ({}^{235}U/{}^{204}Pb)e^{\lambda 235t-1}$$

$$\textbf{(3)}\quad ({}^{208}Pb/{}^{204}Pb) = ({}^{208}Pb/{}^{204}Pb)_0 + ({}^{232}Th/{}^{204}Pb)e^{\lambda 235t-1}$$

(Bourdon *et al*., 2003). The ^{238}U and ^{235}U radiometric system is considered to be the most robust chronometers in geology for examining a wide age spectrum across many different lithologies. (Mattinson, 2010).

2.1 U-Pb Geochronology in Zircon

Detrital zircon ($ZrSiO_4$) geochronology is a rapidly developing, important tool for determining the provenance and maximum depositional age in sedimentary systems (Gehrels, 2011). Zircon is a robust mineral and the U/Pb system has two decay systems within it (^{238}U - ^{206}Pb and ^{235}U – ^{207}Pb), which cover almost all geologic time on Earth (Gehrels, 2011). The main cation of zircon is Zr^{4+}, which can be replaced by uranium ($U^{4+)}$. In contrast, Pb ions are are virtually excluded from the zircon lattice during crystallization, thus the mineral is an ideal candidate for U/Pb dating (Gehrels, 2011). In the last decade most zircon has been dated using Laser Ablation Inter-Coupled-Plasma Mass Spectrometers (LA-ICPMS), conducted on a polished crystal surface, yielding an age with precisions ranging from 1-2% (Gehrels, 2011). LA-ICPMS dominates U/Pb dating analysis because of the relatively fast analysis time and low cost (Gehrels, 2011). Gehrels (2011) summarizes the three main incentives historically for dating detrital zircon (1) to characterize provenance; (2) the correlation of sedimentary units if provenance is identical; and (3) determining maximum depositional ages. This technique, however, is not without its disadvantages. Zircon is a prevalent mineral in many igneous, metamorphic, and sedimentary rocks making it an ubiquitous tool for U/Pb dating.

METHODS

U-Pb Geochronology:

Alluvium was sampled from rivers across the Canterbury Plains and the following river drainages: Waipori, Clutha, Catlin's, Grebe, Arawhata, Haast, Paringa, Mahitahi, Makawhio, Karangarua, Wanganui, and Hokitika (Fig. 1, 2, and 3). Every sample was coarsely sieved (<5mm) and a secondary sample at each locality was gold panned to concentrate dense accessory minerals. At Syracuse University, samples were sieved at three size fractions prior to mineral separation: 600-micron, 400-micron, and 250-micron. The 250 micron size fraction was used for the heavy liquid and subsequent processing. Disposable sieve cloth was used to reduce the potential for cross contamination between samples. Mineral separation was performed using a Frantz isodynamic magnetic separator (side slope of 15 degrees and a current of 1.5 A) and running the nonmagnetic fraction of minerals through the dense liquids bromoform (density = 2.85 g/cm^3) first and methylene iodide (density = 3.3 g/cm^3) second. To assess age, grain mounts were made with a dual strategy, random selection grains picked based on color, size, and shape. Combining selective and random grain techniques may better characterize the source regions represented and help assess the validity of detrital mineral characterization as bedrock proxies (Leary *et al., 2019)*. Zircon grains were placed onto double sided tape and mounted in epoxy, ground and polished. They were then imaged on a Gatan MiniCL detector attached to a FEI Quanta 600 SEM at California State University Northridge to determine zoning and heterogeneities.

Uranium-lead isotopic ratios were collected using a ThermoScientific Element2 SF-ICPMS coupled with a Teledyne Cetec Analyte G2 Excimer Laser (operating at a wavelength of 193 nm) at California State University Northridge. Prior to analysis the Element2 was tuned using the NIST 612 glass standard to optimize signal intensity and stability. Laser beam diameter was ~25 microns at 10 Hz and 75-100% power. Ablation was performed in a HelEx II Active 2-Volume Cell™ and sample aerosol was transported with He carrier gas through Teflon-lined tubing, where it was mixed with Ar gas before introduction to the plasma torch. Flow rates for

Ar and He gases were as follows: Ar cooling gas (16.0 NL/min), Ar auxiliary gas (1.0 NL/min), He carrier gas (~0.3-0.5 NL/min), Ar sample gas (1.1-1.3 NL/min). Isotope data were collected in E-scan mode with magnet set at mass 202, and RF Power at 1245 W. Isotopes measured include 202Hg, 204(Pb+Hg), 206Pb, 207Pb, 208Pb, 232Th, and 238U. All isotopes were collected in counting mode with the exception of 232Th and 238U which were collected in analogue mode. Analyses were conducted in a ~40 seconds time resolved analysis mode. Each zircon analysis consisted of a 20-second integration with the laser firing on sample, and a 20 second delay to purge the previous sample and move to the next sample. Approximate depth of the ablation pit was ~20-30 microns.

The primary zircon standard, 91500, was analyzed every 10-15 analyses to correct for in-run fractionation of Pb/U and Pb isotopes. A second zircon standard, Temora-2, was analyzed every ~10 analyses to assess reproducibility of the data. Total uncertainties (analytical + systematic) were determined by the software program Iolite®. U-Pb analysis of Temora-2 during all analytical sessions yielded concordant results and error-weighted average ages of **421.8 ± 1.8 Ma** (2* SE N = 150 grains, 24 discordant grains removed) (Appendix A, Black et al., 2004; Mattinson, 2010). A 5% discordance filter was applied to Temora-2 grain-ages with the percent difference between the $^{207}Pb/^{235}U$ date and $^{206}Pb/^{238}U$ date.

U-Pb isotopic data were plotted using IsoplotR (Vermeesch, 2018). Corrections for minor amounts common Pb in zircon were made following methods of Tera and Wasserburg (1972) using measured $^{207}Pb/^{206}Pb$ and $^{238}U/^{206}Pb$ ratios and an age-appropriate Pb isotopic composition of Stacey and Kramers (1975). Zircon with large common Pb corrections (e.g., analyses interpreted as having ~20% or greater contribution from common Pb) were discarded from further consideration. Preferred zircon dates are reported using the $^{206}Pb/^{238}U$ date for zircon

<1100 Ma, and the ^{207}Pb/^{206}Pb date for zircon >1100 Ma, however all dates are reported in the supplemental data (see appendix).

For detrital zircon, a 10% discordance filter was applied to all data (Appendix B). For zircons >1100 Ma, discordance is calculated as the percent difference between the ^{207}Pb/^{206}Pb date and ^{206}Pb/^{238}U date. For zircons younger than 1100 Ma, the ^{207}Pb/^{206}Pb date is an unreliable indicator of discordance due to low abundances of measured ^{207}Pb. For these zircon crystals, discordance is calculated as the percent difference between the ^{207}Pb/^{235}U date and ^{206}Pb/^{238}U date.

ArcGIS:

Watersheds for every sample location were delineated using ArcGIS. First a 25 m New Zealand Digital Elevation Map (DEM) was imported to Arc GIS Pro from the New Zealand government GIS site (Fig. 4) (https://lris.scinfo.org.nz/data/tag/dem/global/oceania/new-zealand/?s=ar). Then the raster to mosaic tool was used to make one continuous DEM for the entire South Island of New Zealand. This DEM was used to blend the target raster tiles (DEM tiles from New Zealand Government: Environment and Land LRIS Portal). DEMs were used from the Global Multi-Resolution Topography (GMRT) online tool and New Zealand Digital Elevation Map from the Land Resource Information Systems (LRIS) online portal at 90m and 25m resolutions. To make sure data were not lost, multiple different DEM resolutions were tested to map watersheds, including a 9m, 25m and 110m DEM. For the final overall analysis, the 25 m GMRT DEM was used as its resolution is still finer resolution than the 250,000:1

geologic map used for this study and requires significantly less computational time per watershed.

All the negative elevation values needed to be removed by using the raster calculator tool with the SetNull expression: *SetNull(“elev” < 0, “elev”)*. This creates a raster that does not display any bathymetry. For the purposes of this study, it was inconsequential to extend watersheds into the ocean basins. Following this, the flow direction geoprocessing tool was used to delineate flow direction of water droplets on the land surface. This tool assigns a flow direction to each raster pixel within the raster. This raster is then input into the flow accumulation geoprocessing tool. The flow accumulation tool builds on this, identifying where the drainages flow. At this step it was crucial to make sure each sample was placed in a specific drainage. The watershed geoprocessing tool was employed to map the watersheds upstream of the samples. To calculate the percentages of geologic terranes within the watersheds, the geologic map from Geological Nuclear Survey (GNS) science of New Zealand was clipped and then the intersect tool was used to extract a table. For simplification of viewing the maps, only 11 major geologic terranes and the Median Batholith were included within the percentages (See Figures: 5 and 6).

Statistical Analysis

Probability density plots (PDPs) were created in Microsoft Excel® to model grain-age distributions across all alluvium samples. Each sample was initially evaluated by comparing grain-age peak distributions across the samples. PDPS were made looking at both the Precambrian and Cambrian-Present (500 – 0

$$D = \frac{\max}{-\infty < x < \infty} \left| S_{N_1}(x) - S_{N_2}(x) \right|$$

Ma). The Kolmogorov-Smirnoff (K-S) test allows for the comparison of two discrete populations to determine whether they are statistically different (Lovera *et al*., 2008). Specifically, the K-S test evaluates the validity of the null hypothesis, which is that there is no statistical difference between two populations and any difference is due to sampling error or poor sample size (Press *et* al., 2002). The null hypothesis is evaluated by taking the difference between the absolute value between two cumulative density functions (CDFs) (Lovera *et al*., 2008). This is known as the two sample KS test and can be defined as: $+S_{N1}$ (x) and S_{N2} (x) are different data sets for the CDFs and (x) is the known distribution function (Lovera *et al*., 2008). This was employed to ascertain whether detrital samples are accurately measuring the geological terranes they are draining. This method has been widely used for interpreting detrital zircon (e.g., Dickinson and Gehrels, 2009; Miller *et* al., 2013 and references therein). The critical measure of the test is the P-value. If the P-value is greater than 0.05, there is 95% confidence the two populations are the same. K-S testing was performed using the University of Arizona Laserchron KS test Excel Macro.

Following the methodology of Saylor and Sundell (2016), DZStats, a MATLAB based code was used to perform additional statistical analysis. The following statistical tests were employed: Cross-correlation, Likeness, Similarity, K-S with a p value (See above), K-S D statistic, and Kuiper test. A robust statistical test according to Saylor and Sundell (2016) should: (1) maximize the sensitivity by using the full range of coefficients. (2) The degree of similarity between samples derived from the same population should increase with increasing sample size. (3) Sample specific complexities should be minimized by the statistical test. The Kuiper test, like the K-S test, tests the null hypothesis that two samples are drawn from identical parent populations (Press *et al*., 2007). The Kuiper V test is calculated using two CDFS (F_1 and F2)

(Saylor and Sundell, 2016). As with the K-S test a p-value <0.05 says with > 95% confidence that the two samples are not drawn from the same parent population. The K-S and Kuiper tests, however, both require large sample sizes to accurately reject the null hypothesis.

The likeness test (Satkoski *et al*., 2013). was used to evaluate and compare against the K-S test. The likeness test determines how alike two populations are. Likeness, similar to the Gehrels (2000) similarity metric, utilizes all the information in a Probability Density Plot (PDP) (Satkoski *et al*., 2013). With the likeness test, higher values indicate greater similarity.

Final interpretation was done using the Cross-correlation coefficient of determination—a cross-plot of PDPs and/or Kernal Density Estimates (KDEs) of two samples from the same age interval (Saylor and Sundell, 2016). The cross-plot is advantageous because it can distinguish the absence or presence of age peaks relative along with changes in magnitude. If two samples have an identical grain-age distribution, the Cross-correlation coefficition (R^2) value would be 1. If there is zero overlap in the grain-age distribution the (R^2) value would be zero (Saylor and Sundell, 2016).

RESULTS

Watersheds were delineated for all the original sample locations. Due to low zircon yield only 13 samples were dated out of the original 26 samples, with N = 437 concordant grains examined in the Western Province and N = 529 concordant grains in the Eastern Province. Sample size ranged from 30-100 grains dated per sample. Eleven different geologic terranes were examined within the watersheds upstream of the sample locations. For the Western Province the: the Buller and Takaka Terranes and the Median Batholith. In the Eastern Province the Caples, Dun Mountain, Murihiku, Pahau, Rakai, Kaweka, Waipapa, Drumduan, and the

Brook Street terranes were assessed in the watersheds for their grain-age contributions (Tables 1 and 2 and Fig. 4). These terranes were chosen because they represent the largest aerial exposures in the mapped watersheds (Fig. 1). Sample 20SOZ-03 is from the largest watershed, encompassing an area greater than 20,000 km^2 (See Fig. 4). The Caples and Waipapa terranes dominated the exposed aerial percentages of the geologic terranes within the watersheds, accounting for over 50% of them (Tables 1, 2, and 3, Fig. 3, 4, 5, and 6). The Brook Street Terrane, Kaweka Terrane, and Drumduan Terrane represent the smallest percentages of the watersheds (Fig. 1 and 4).

Of the 26 samples, 13 samples that yielded enough DZ for U-Pb dating (N= 1,101) (see Table 4; Fig. 1, 5, and 6) it is the Triassic through Carboniferous (360-200 Ma) grain-age component comprises the preponderance of grains in the samples (Table 2). Samples were subdivided by placing them in the Western and Eastern Provinces. The Western Province samples generally yield younger zircon, but both provinces have a large age peak at 260 Ma and 120 Ma (Fig. 10). Only samples 20SOZ-15, 16, and 19 have a significant Precambrian (2600-542 Ma) detrital zircon component (See Table 3). Two of the dated samples, 20SOZ-01 and 20SOZ-21, have more than a 25% input of Early Cretaceous (146-100 Ma) grains (Fig. 10 and Table 3). All the samples were statistically compared against the basement rocks of the Western and Eastern Provinces from six different published data compilations. Adams *et al.*, (2015) was used to "represent" the Western Province. For the Eastern Province, three published grain-age compilations were used: Campbell *et al.*, (2020) **A**, Campbell *et al.*, (2020) **B**, and Campbell *et al.*, (2020) **C**. To account for recent volcanism and modern alluvium input Adams *et al.*, (2007, 2015, and 2017) was compared against the eastern province samples in this study. The Adams data sets were chosen because they represent a large compilation of sedimentary accretionary prism and backarc terrane lithologies across the Buller, Takaka, Brook Street, Murihiku Supergroup, Dun Mountain-Maitai, Torlesse supergroup, and Caples terranes across the Western and Eastern Provinces (Adams *et al*., 2007 and Adams *et al.*, 2015).

The grain-age distributions were all dominated by a Late Cretaceous signal around _90-120 Ma (Fig. 7). The samples in the Eastern Province have a larger Late Cretaceous grain-age distribution peak compared to the Western Province (Fig.7).

To statistically elucidate whether the alluvial samples were faithfully representing the crystalline basement rock or sedimentary terranes they are draining, they were compared against all these data sets using the K-S, likeness, Similarity, Kuiper, and Cross-correlation statistical tests (Tables 4, 5, 6A, 6B, 7, 8, and 9). K-S and Kuiper tests –using both the Laserchron excel workbooks for the K-S tests and Saylor and Sundell DZStats MATLAB workbooks—yielded one sample (20SOZ-07) that is not statistically different from the sedimentary bedrock compilations: the Adams accretionary compilation and the Campbell *et al*., (2020) **B** compilation (Tables 6 and 7). The likeness test comparison, however, yields many more samples with >50% likeness to at least one of the published grain-age compilations. Samples 20SOZ-02, 03, 07, 08B, 11B, 12, 13, 14, 15, and 19 all have > 50% likeness to at least one grain-age compilation. Samples 20-SOZ-14, 15, and 19 display >50% likeness with only the Adams *et al*., (2015) compilation (Table 9). The rest of the samples display >50% likeness with the Campbell *et al*., (2020) **A**, Campbell *et al*., (2020) **B**, and Campbell *et al*., (2020) **C,** and Adams accretionary compilation, but not the Adams *et al*., (2015) compilation (Table 9). The same is seen with the Cross-correlation coefficient determination. None of the samples have a >0.5 R^2 value for the Adams *et al*., (2015) Buller and Takaka compilation (Table 8).

All the DZ samples were compared against a plutonic bedrock compilation with N=337 grains across the Zealandia cordillera using KS testing (Kimbrough and Tulloch, 1989; Kimbrough et al., 1994; Muir et al., 1996; Waight et al., 1997; Ireland and Gibson, 1998; Muir et al., 1998; Davids, 1999; Tulloch and Kimbrough et al., 1999; Tulloch and Kimbrough et al., 2003; Allibone and Tulloch, 2004; Gollan, 2006; Price et al., 2006; Bolhar et al., 2008; Scott and Palin. 2008; Tulloch et al., 2009; Turnbull et al., 2010; Tulloch et al., 2011, Turnbull et al., 2013; McCoy-West et al., 2014; Allibone et al., 2016; Decker, 2016; Martin et al., 2016; Schwartz et al., 2017; Van der Meer et al., 2018; Buriticá et al., 2019; Ringwood *et al.,* 2021). The compilation encompasses crystallization ages of rocks in: Fiordland, Stewart Island, NW Nelson-Buller, The Longwood Range, Westland, and West Coast-Buller. Zircon U/Pb ages, for this compilation, represent igneous rocks in the Zealandia Cordillera formed between 500-100 Ma (Fig. 10). KS statistical analysis was performed following the same methodology as with the sedimentary terrane compilations of Zealandia. None of the modern detrital samples statistically matched the plutonic bedrock compilation using the K-S and Kuiper tests (i.e. they failed the null hypothesis that the bedrock ages and DZ ages appear to be from the same population). When the same comparison is made using the Cross-correlation coefficient of determination, two samples have a > 0.5 R^2 value: 20SOZ-01 and 20SOZ-21 (Table 10). These are the only two samples, that do not have a > 0.5 R^2 value compared against the sedimentary grain-age compilations (Table 8).

DISCUSSION

Alluvium from across the South Island, New Zealand, was sampled draining from every major lithotectonic terrane (Fig. 1, 5, and 6). Watersheds were mapped upstream of each sample dated (see Fig. 5 and 6). Based on the exposed aerial percentages of the bedrock within each watershed, one could attempt to predict the grain-age distribution expected in each sample. For example, Samples 20SOZ-14 and 15, both located within the Western Province, have a >10% areal exposure of the Buller terrane located within their watersheds (Fig. 6 and Tables 1 and 2). When comparing 20SOZ-14 and 15 against Adams (2015) Buller and Takaka grain-age compilation (N=349) the K-S test does not suggest the samples are from the same source population (Table 6B), i.e it fails the null hypothesis. When the same test is performed with the likeness metric, an interesting change occurs. The likeness test suggests that 20SOZ-14, 15, and 19 are getting 52, 58, and 52% of their grain-age distribution, respectively, from the Buller or Takaka terranes (Table 9). These samples, however, do have small sample sizes: N= 100, 97, and 84, respectively (Table 2). When performing the same test with the Cross-correlation coefficient of determination, the samples fail the null hypothesis and appear to be from different populations (Table 8). This may be the result of a sample size that is not large enough. Saylor and Sundell's (2016) findings with synthetic data sets may help elucidate this studies DZ statistical trends. Saylor and Sundell (2016) found with synthetically generated data sets, a PDP Cross-correlation coefficient value greater than 0.64 for N=500 grains, the two sub samples must be derived from identical populations. Alternatively, with two smaller sub samples of N = 100, Saylor and Sundell (2016) found that derivation from an identical source (or a different but closely related source) cannot be elucidated definitively. Samples 20SOZ-14, 15, and 19 could be behaving as the synthetic N =100 sub-samples. The likeness test might suggest at least a proportion of these grains are being derived from the Buller and Takaka terranes, yet the sample size is too small to confidentially resolve the Cross-correlation coefficient values. The difference in remaining grains could be not well documented recycled zircon, possibly of Gondwanan origin.

In the Eastern Province, seven of the dated samples—20SOZ-1, 2, 3, 7, 8B, 19, and 21—failed the K-S test when comparing against the Campbell *et al*., (2020) **A**, Campbell *et al*., (2020) **B**, and Campbell *et al*., (2020) **C** grain-age compilations. The **A** Campbell grain-age compilation is used because it represents Permian-Triassic fore-arc terranes like the Eastern Province Central Arc terranes: Brook Street, Murihiku, Kaka Point Structural Belt, and the Dun Mountain-Maitai. The Campbell **B** grain-age compilations is comprised solely of Murihiku terrane grains. The last grain-age compilation, Campbell **C**, was used because it is the largest compilation of Eastern Province central arc and accretionary prism terrane grain-ages. When performing the same comparison as the K-S test, but with the likeness metric, all the Eastern Province samples except 20SOZ-01 and 20SOZ-02, coincide with >50% of their grain-age distribution from at least one of these Eastern Province Compilations (Table 9). When performing the same comparison with the PDP Cross-correlation test, all the Eastern Province samples except 20SOZ-21, have a PDP Cross-correlation value >0.5 for at least two of the Eastern Province Compilations (**A, B, C**; Table 8). Unlike with the Western Province samples, there is agreement between the Cross-correlation and likeness tests in the Eastern Province. Perhaps that even with smaller sample sizes (See table 2) compared to larger bedrock grain-age compilations, there is significant overlap. The three Campbell grain-age compilations likely well represent a significant portion of the original source for the Eastern Province samples 20SOZ-01, 2, 3, 7, 8B, and 19. These statistical test results corroborate the findings of Saylor and Sundell (2016). Small sample sizes compared to large source populations does not work well with the K-

S and likeness tests. The sample is overrepresented and the source population is under represented.

Sample 20SOZ-21 is the only sample that fails all the statistical tests compared to large Eastern and Western Province grain-age compilations. It is draining a watershed that is comprised of 100% exposed Pahau Terrane, the easternmost component of the Torlesse Composite Terrane (Mortimer *et* al., 2014; Edbrooke, 2017; Fig 6). Using the likeness statistical test, 20SOZ-21 has only a 37% likeness between the sandstone bedrock and the modern DZ (Table 6). Therefore, ~63% of the modern DZ signal is not well documented in DZ record of the Pahua terrane. Since the Pahua terrane is a large sedimentary package, with varying degrees of metamorphism, a large proportion of the grains are almost certainly recycled and have not been well characterized yet. These grains are likely linked to Gondwanan continental-margin growth, prior to the rifting and formation of Zealandia –which have not yet been well dated in the literature. The modern alluvium 20SOZ-01 (N=100), does not well represent the catchment that it is draining. A more specific comparison to the Pahua terrane may be needed, or simply the Pahua terrane's grain-age distribution has not yet been fully characterized. The small sample size (N = 100) compared to large data sets, however, could also be leading to the failure of the statistical tests. All these factors are likely contributing to the results of this comparison. Additionally, Sample 20SOZ-21 likely has a median batholith input that is contributing to the younger grain-age distribution (Fig. 7). For example, Sample 20SOZ-01 is the only sample draining Fiordland directly and has a >.5 R^r value compared against the plutonic compilation (Table 10).

Modern alluvium in catchments is showing a larger grain-age distribution than what is currently known in the bedrock they are draining. Modern sediment should, ideally, display a one-to-one relationship compared to the bedrock it is draining. We can think of two possible explanations for this unaccounted-for signal in the bedrock today. The first, and perhaps most likely, is the current bedrock needs more characterization as it may be considerably more heterogenous than previously thought, i.e., there are unidentified pluton and/or sedimentary formations that could be contributing these zircons. A second, and speculative suggestion, is that the unaccounted for Precambrian detrital zircons in the modern alluvium could be wind-blown. Zircon has been documented in loess deposits and can be entrained in the wind (Dickinson *et* al., 2011; Nadin *et al*., 2022). We cannot disprove this second idea at this time, but it seems unlikely that zircon could be blown hundreds to thousands of kilometers externally contaminating our studied alluvium (Dickinson and Gehrels, 2009). It is more likely that the bedrock is not as well characterized as thought and is more heterogeneous than previously assumed. For example, this study compared samples against six large grain-age distributions—Adams (2015), Adams accretionary compilation, the plutonic compilation, and Cambell **A, B, and** C—have N = 349, 359, 152, 446, 935, and 446 dates respectively—and were not fully represented in the bedrock. The >1000 grains in this study show grain-age distributions not seen in some of New Zealand's largest sedimentary bedrock and plutonic grain-age compilations (Fig. 10 and 9).

Within the Zealandia cordillera, it is dominated by two high magma-addition-rate (MAR) events (Ringwood *et al.*, 2021). One, during the Devonian, between 370-368 Ma and a second during the Early-Cretaceous, between 129-105 Ma (Ringwood *et al*., 2021). These events are well represented in the Sedimentary bedrock grain-age compilations used in this study (See Fig. 10). For both the Western and Eastern Provinces, there is an abundance of grain-age distribution between 360-200 Ma (Fig. 10). Both provinces have a large peak at 260 Ma and 120 Ma (Fig. 10). The 120 Ma peak could be contributed to this second MAR event documented in the New

Zealand Cordillera. The large grain-age distribution centered around 360-200 Ma, further supports a narrative of long-lived Gondwanan recycling that is not well documented in New Zealand sedimentary bedrock (Fig. 10 and 9). Zircon recycling would help to explain the likeness and cross-correlation coefficients of determination not being higher, i.e., there is an unaccounted for component in the source population.

It's known that changes in river incision and where sampling occurs can bias DZ age distributions. Studies of the Amazon River (Mapes *et al.*, 2004, 2005) and Frankland River of Australia (Cawood *et al*., 2003) observed a predominance of proximal zircon sources over much larger sources in the drainage. For instance, the Yilgarn Craton underlies 70% of the Franklin River in Australia, but downstream only comprises 25% of the DZ grain-age spectra (Cawood *et al*., 2003). Similarly, our alluvial samples might not be a good representative of the major bedrock units in a particular terrane, but may be dominated by more local, as yet unidentified, or not well characterized, sources. In fact, based on our data one might well predict that there are still sedimentary formations, plutons, and/or metamorphic units yet to be documented within the watersheds of this study. Alternatively, there is a preponderance of recycled zircon grain-age populations that need to be better characterized within the units already mapped.

In this study, between 30 and 100 DZ grains were analyzed per sample (Table 2). Some samples had extremely low zircon yields and thus the N-value is well below what is now expected in DZ studies. Yet sample size alone cannot be the solution as we have found a *larger* age spread in DZ grains than what is currently known about bedrock ages in many of the catchments. If the opposite were true, i.e., many more age populations in a specific bedrock region were known compared to those identified by DZ analyses of modern alluvium, then DZ sample size could be the main explanation. But that is clearly not the case in this study. In some instances (i.e. 20SOZ-01), less than 100 DZ grains were analyzed, yet the grain-age distribution is more extensive than that of the watershed's source terrane and does not statistically match a diverse sedimentary and plutonic bedrock compilation (Tables 2, 8, and 9).

CONCLUSIONS

The study of DZ and bedrock comparison (both igneous/metaigneous and sedimentary/metasedimentary) typically assumes that the percentage area of terranes in a watershed is the primary factor influencing the age spectra of zircons within a sand sample. DZ geochronology has become the primary tool for elucidating sedimentary provenance, however, with its rapid acceptance many biases have been overlooked or unrecognized. In analyzing 13 U-Pb DZ samples from modern alluvium across the South Island, New Zealand, watersheds with the aerial percentages of the 11 largest geologic terranes were mapped. Through K-S, Likeness, Kuiper, and Cross-correlation coefficient statistical testing—compared to five large sedimentary bedrock grain-age compilations and a plutonic grain-age compilation—we have demonstrated that there is significant percentage of the samples not accounted for in the bedrock compilations. The highly refractive nature of zircon and resilience to physical/chemical break down allows it to be recycled multiple times. Unaccounted DZ in these statistical tests likely represent older Gondwannan grain-age populations in the alluvium, that have not yet been characterized in the bedrock. This epitomizes the prevalence of zircon recycling. Changes in erosional rates, laterally and through time, coupled with dynamic sediment transport likely further increase differences between the alluvium and parent lithologies. These factors would only be amplified in the metasedimentary-sedimentary exposed bedrock today. If DZ in Modern alluvium does not match the bedrock how amplified do these biases become when examining ancient sedimentary units?

This study used the South Island, New Zealand, as a natural laboratory to examine provenance bias to test the complications of DZ sedimentary provenance. DZ interpretations need to take into consideration how well characterized the parent bedrock is when making provenance assumptions and interpretations. Increasing the number of grains in provenance studies may help alleviate some of these problems, but it is not a comprehensive solution. Even with small grain-age populations, we have demonstrated signals absent in the currently examined bedrock. The bedrock needs to be further characterized. If no further age distributions are found, then we must turn back to the idea of unaccounted zircon being eolian grains.

Detrital zircon is an important tool for constraining some aspects of tectonics and sedimentary provenance, but it needs to be interpreted cautiously in assuming a one-to-one relationship between potential bedrock source and sedimentary sink. Perhaps a better approach would be to include U-Pb dating of multiple accessory minerals to better elucidate tectonic events. It is not yet known if including additional minerals would show similar biases in geochronologically-based provenance analysis in the South Island, New Zealand and elsewhere.

Figures

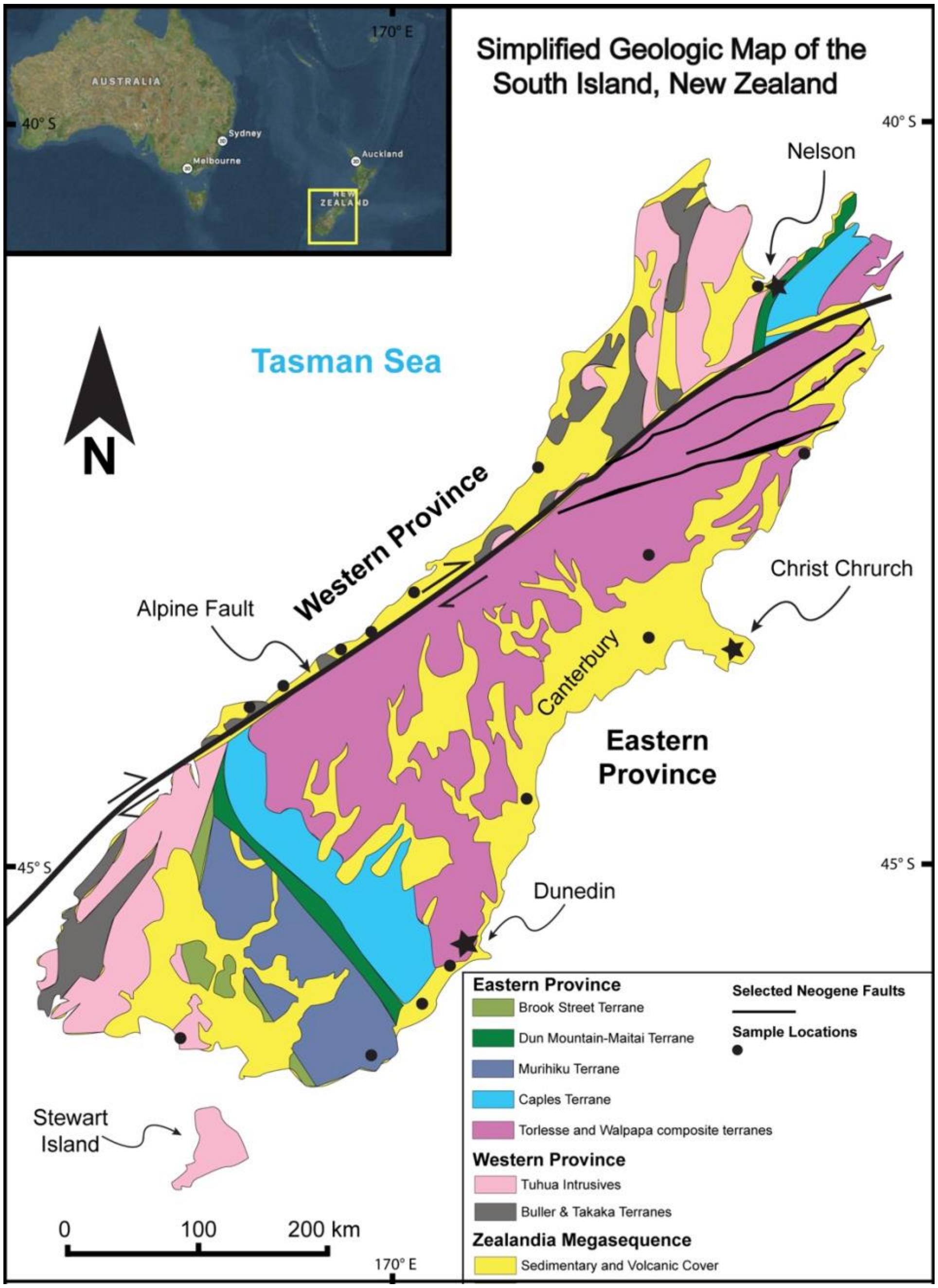

Figure 1: Simplified geologic map of the South Island New Zealand: Eastern province simplified showing the Brook, Dun Mountain-Maitai, Murihiku, Caples, and Torlesse composite terranes. The Western province (west of the Alpine Fault) is comprised of the Buller and Takaka terranes. Sample locations ring the island, located at the mouths of major drainages. Source:

GNS Mapping project (Note: Map is in color, and not all geologic terranes were included for simplicity).

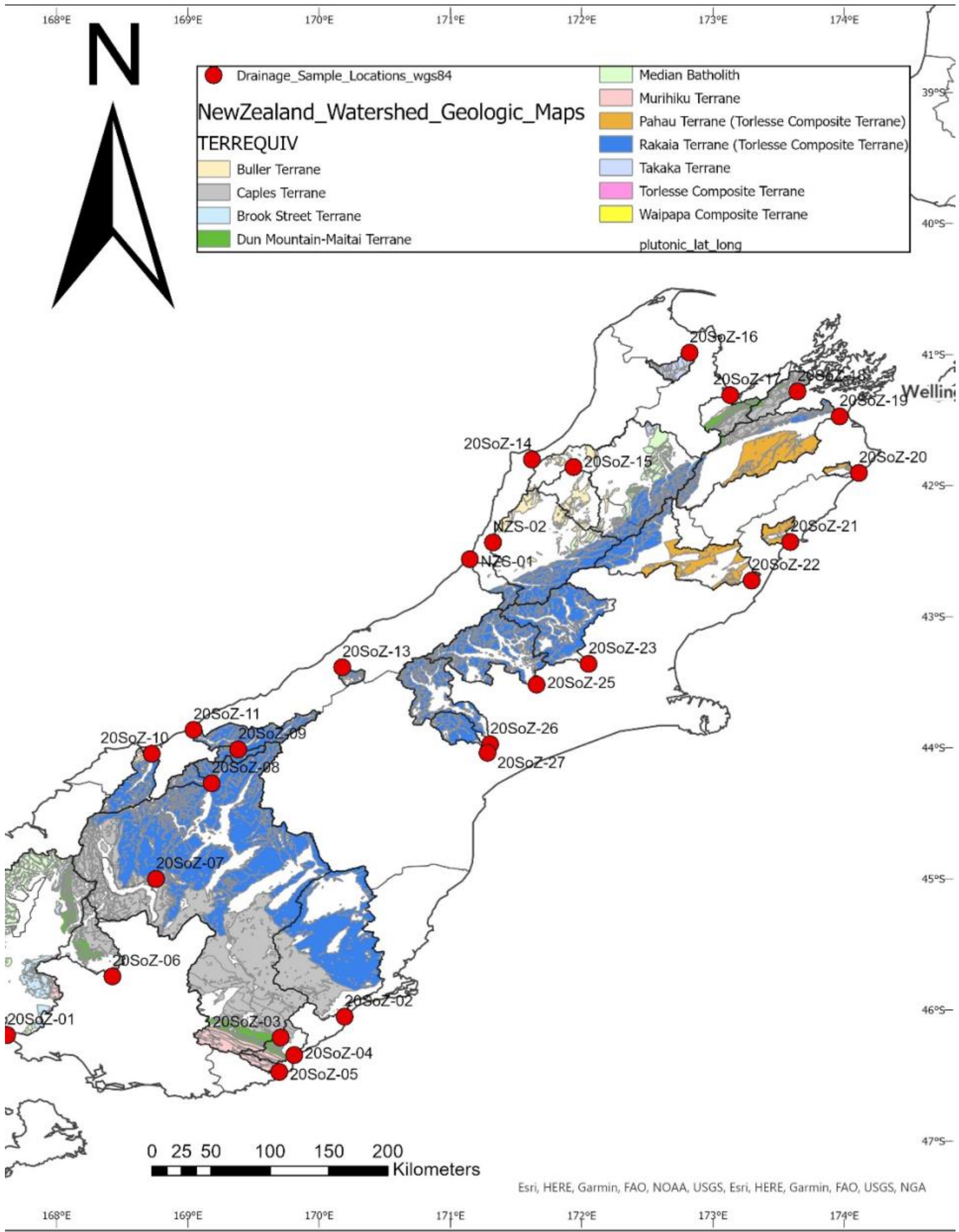

Figure 2: Sample map of spring 2020 field season with sampled drainages delineated by red circles. Up stream of every sample, watersheds are mapped with the dominant geologic terranes exposed within. 13 of 29 samples were U-Pb dated.

Figure 3: 20SOZ-11 Sampling location. Coarse grained sand deposits were prioritized as seen in the foreground of the photo. Sampled within red box.

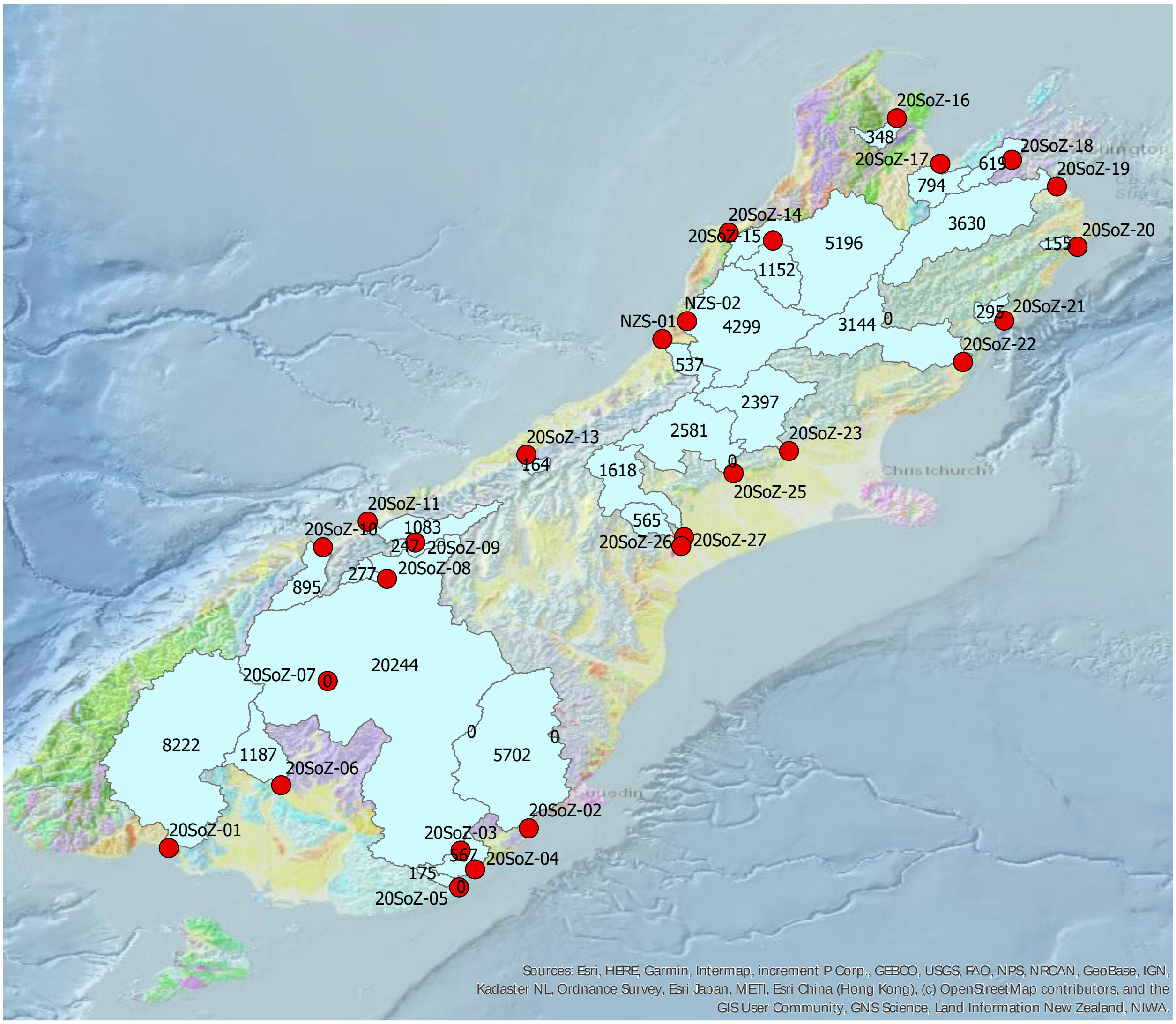

Figure 4: Samples (red circles) and the watersheds they're draining (Blue shade). Numbers in the center of the watershed represent the area of the watershed in km^2 across the South Island, New Zealand. These watersheds were delineated using a 110m resolution DEM from GMRT.

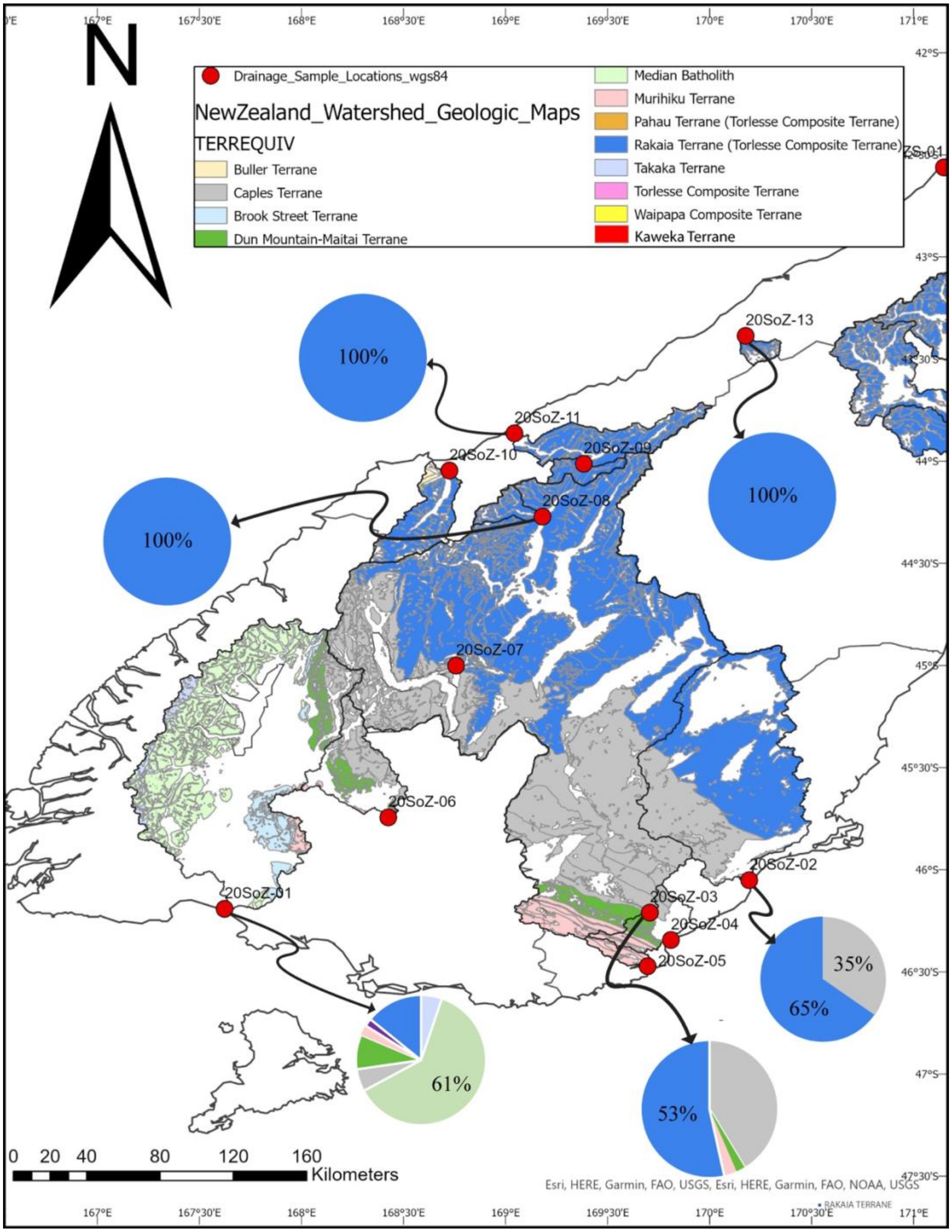

Figure 5: Watershed sample map for southwest corner of the South Island, New Zealand, with pie graphs of the aerial percentages of the 12 largest terranes within each watershed upstream of the specific sample.. Legend indicates the geologic terranes for the pie charts. Red circles represent sample locations and upstream outlined in black are the watersheds.

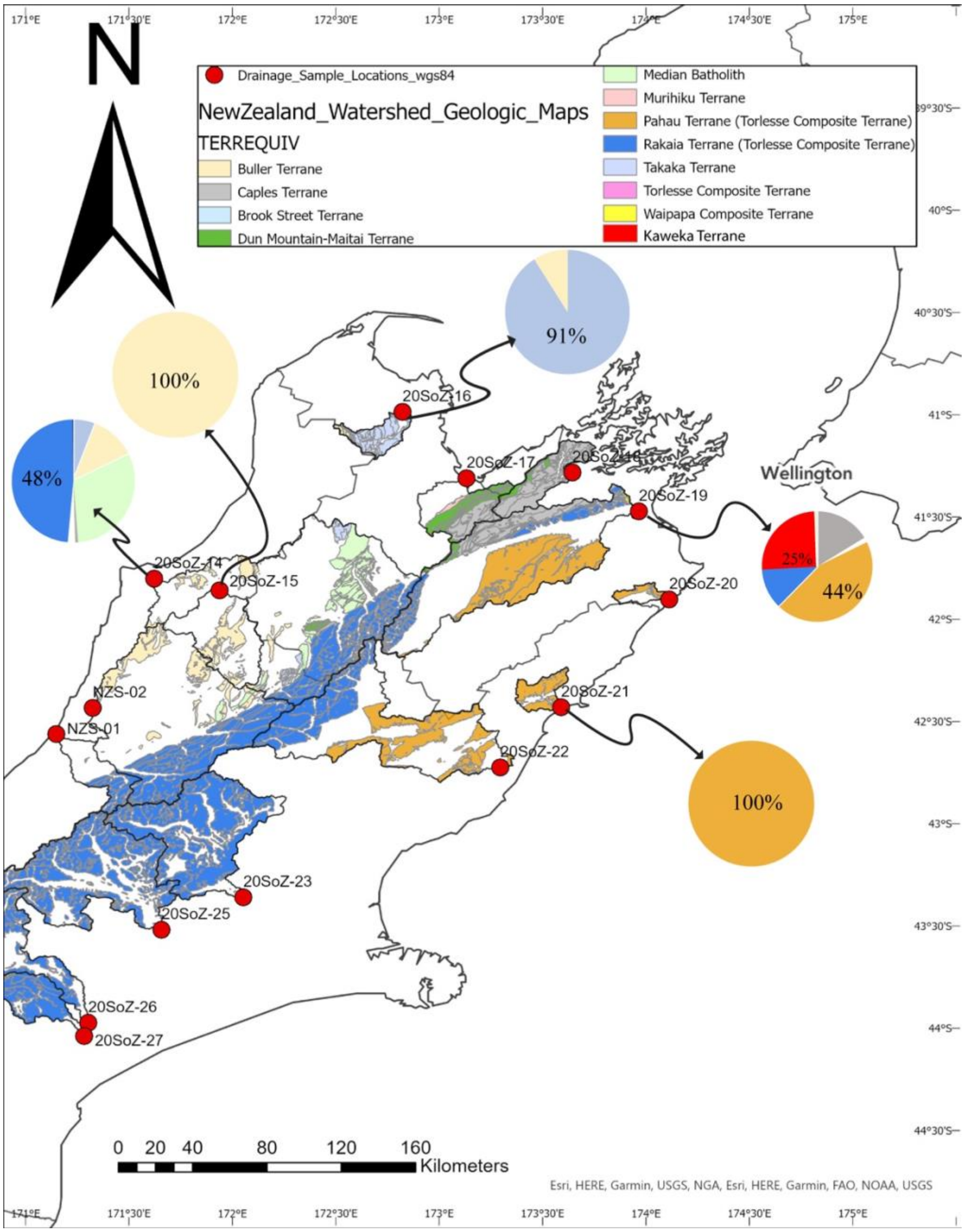

Figure 6: Watershed sample map for Northeast corner of the South Island, New Zealand, with pie graphs of the aerial percentages of the 12 largest terranes within each watershed upstream of the specific sample. Legend indicates the geologic terranes for the pie charts. Red circles represent sample locations and upstream outlined in black are the watersheds.

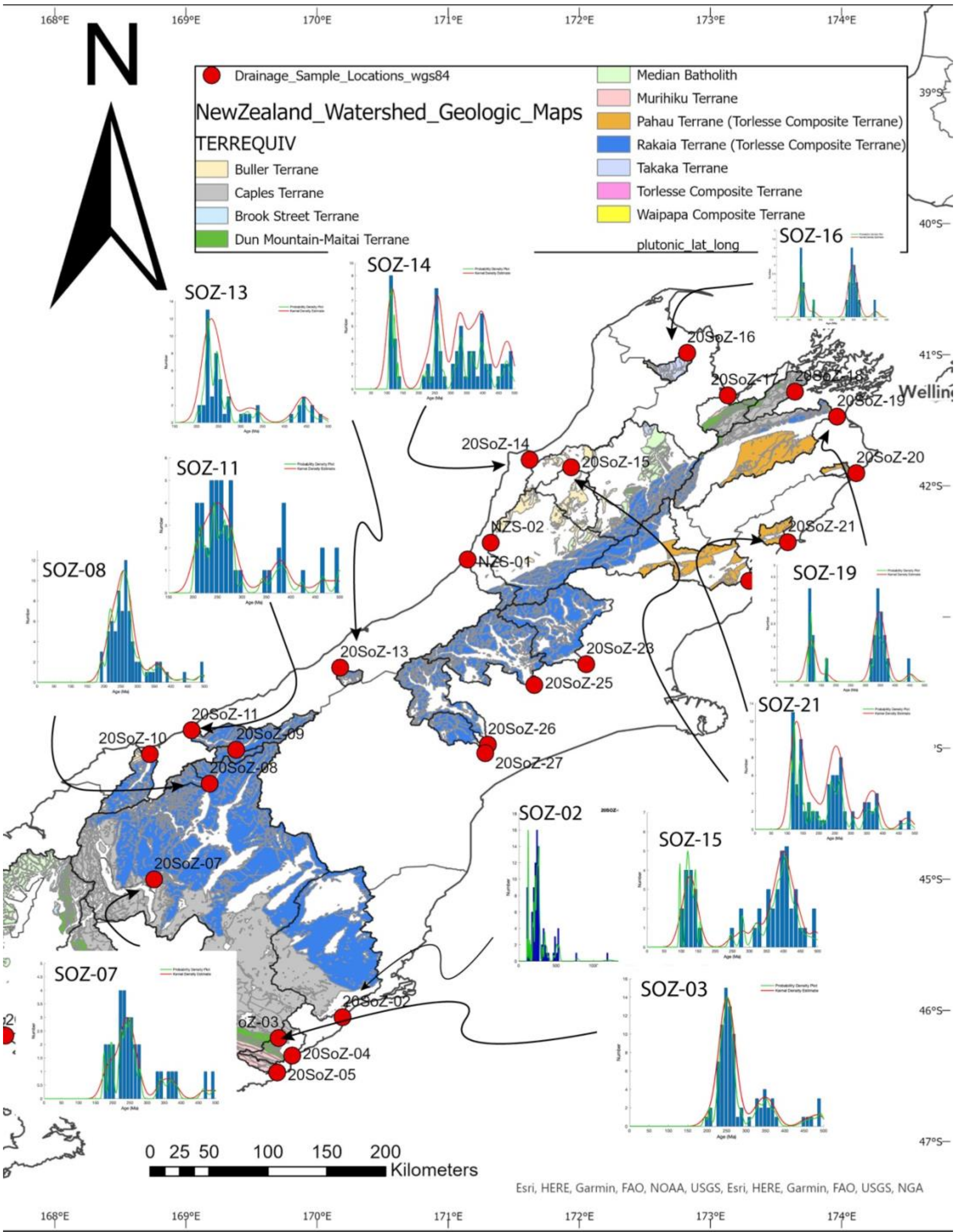

Figure 7: Watershed map of the South Island, New Zealand, clipped to the geologic terranes within each watershed. PDP (red) for each U-Pb dated sample displayed with histogram and kernel density estimate (Green) displayed as well.

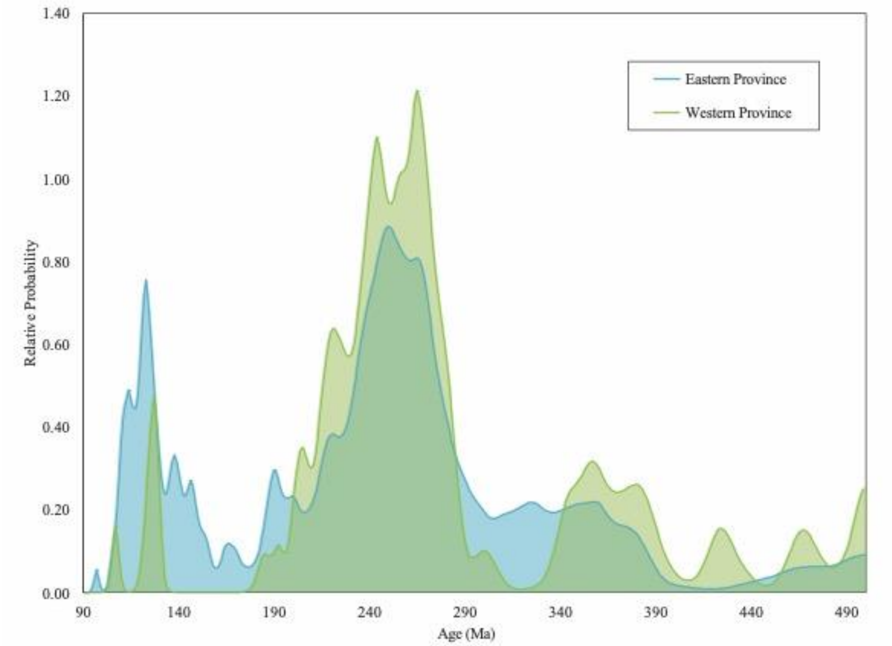

Figure 8: PDP comparison of the sum of the Western (Green N = 437) and Eastern (Blue N = 529) Province grain-age distributions.

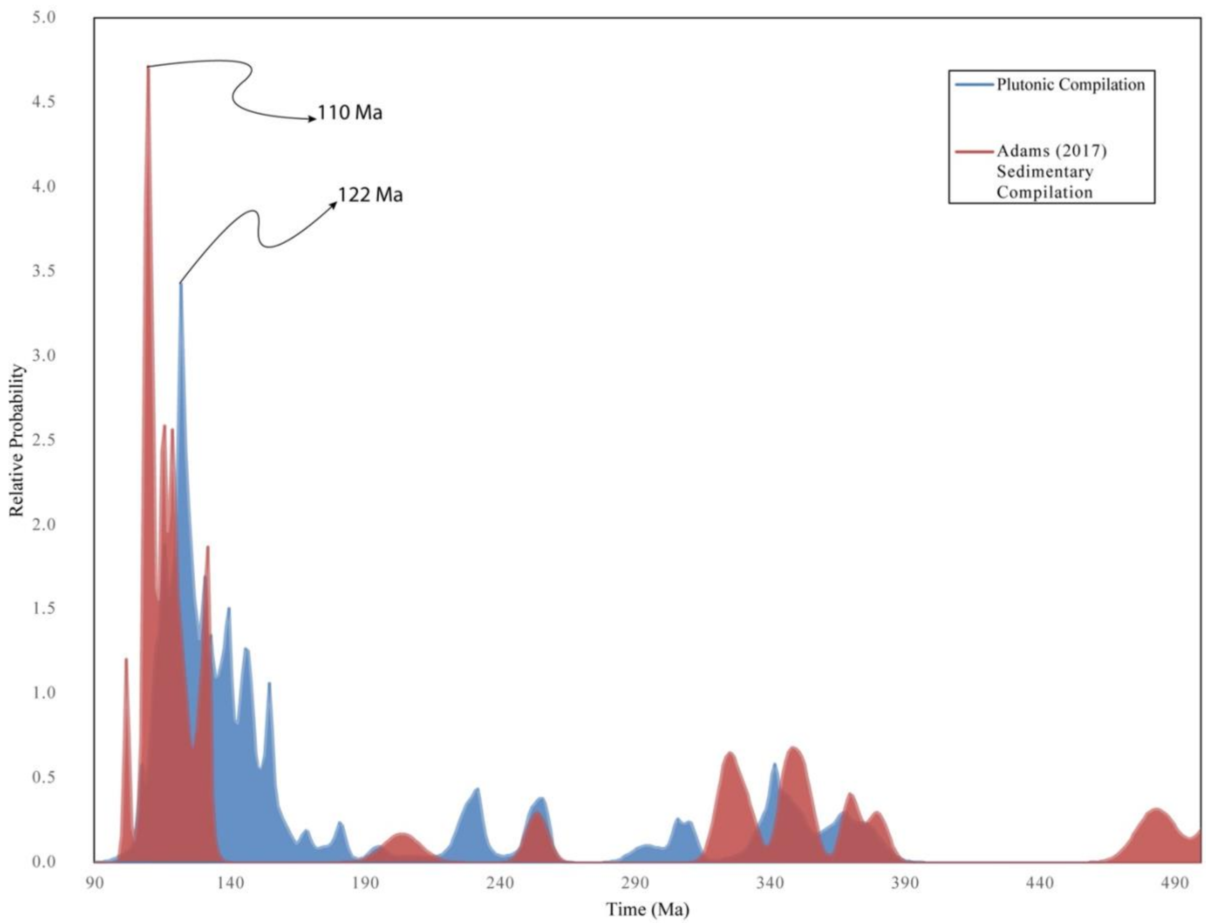

Figure 9: PDP comparison between Adams (2017) DZ compilation and plutonic compilation of 337 igneous crystallization U/Pb zircon ages compiled from: Kimbrough and Tulloch, 1989; Kimbrough et al., 1994; Muir et al., 1996; Waight et al., 1997; Ireland and Gibson, 1998; Muir et al., 1998; Davids, 1999; Tulloch and Kimbrough et al., 1999; Tulloch and Kimbrough et al., 2003; Allibone and Tulloch, 2004; Gollan, 2006; Price et al., 2006; Bolhar et al., 2008; Scott and Palin. 2008; Tulloch et al., 2009; Turnbull et al., 2010; Tulloch et al., 2011, Turnbull et al., 2013; McCoy-West et al., 2014; Allibone et al., 2016; Decker, 2016; Martin et al., 2016; Schwartz et al., 2017; Van der Meer et al., 2018; Buriticá et al., 2019; and Ringwood *et al.,* 2021). Representation of the igneous rocks present in the Zealandia Cordillera.

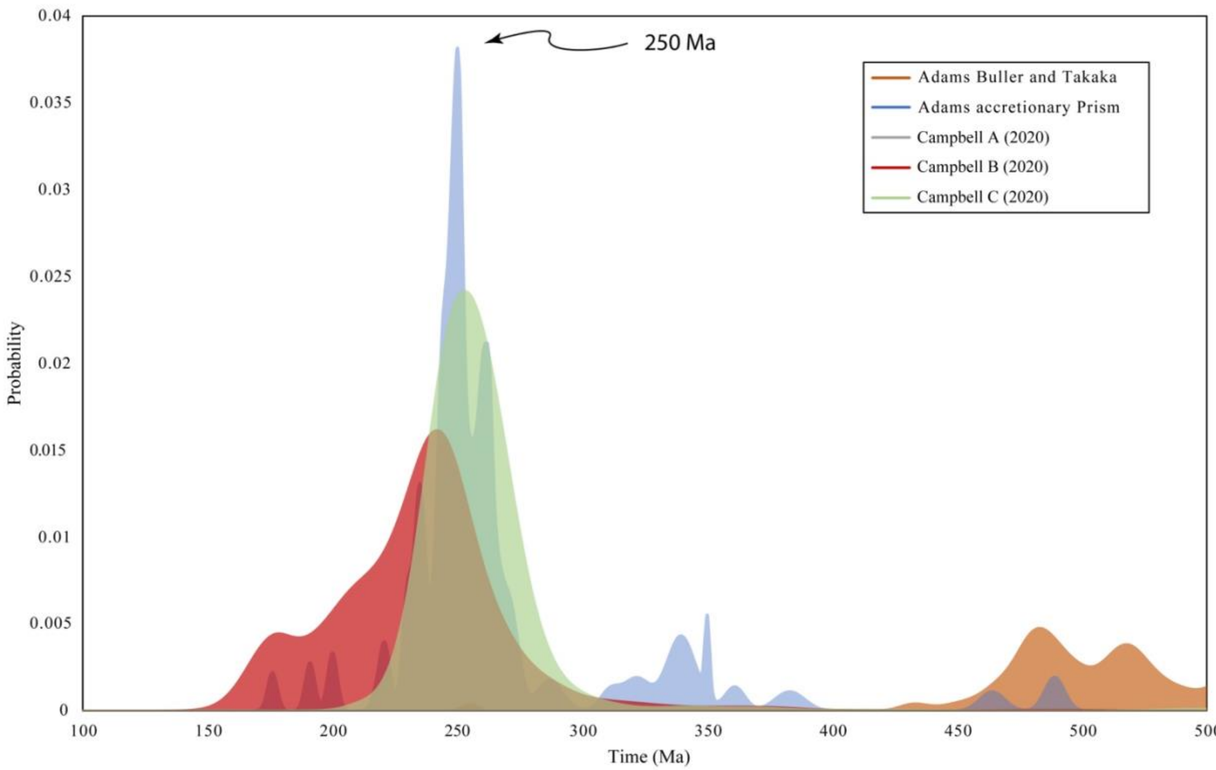

Figure 10: PDP comparison between 5 major sedimentary bedrock comparisons: Adams (2015), Adams accretionary compilation, and Cambell **A, B, and** C—have N = 349,152, 446, 935, and 446 respectively. Major peak for the Adams accretionary Prism compilation (2017) occurs at 250 Ma. Note this is a very small probability for 100-550 Ma. Additionally, the 360-300 Ma is absent, which is present in the samples of this study.

TABLES

Table 1: Percentages of geologic terranes located within each sample watershed. Note, alluvium was removed from this calculation so this is not an aerial percentage.

SAMPLE #	TAKAKA TERRANE	BULLER TERRANE	MEDIAN BATHOLITH	CAPLES TERRANE	DUN MOUNTAIN TERRANE	MURIHIKU TERRANE	PAHAU TERRANE	RAKAIA TERRANE	KAWEKA TERRANE	WAIPAPA TERRANE	DRUMDUAN TERRANE	BROOK STREET TERRANE
Eastern Province:												
20SOZ-01	5.23	0.00	61.93	5.57	8.64	2.50	0.00	0.00	0.00	0.00	1.93	14.20
20SOZ-02	0.00	0.00	0.00	34.66	0.00	0.00	0.00	65.34	0.00	0.00	0.00	0.00
20SOZ-03	0.00	0.00	0.00	41.35	2.13	3.04	0.00	53.48	0.00	0.00	0.00	0.00
20SOZ-08	0.00	0.00	0.00	0.00	0.00	0.00	0.00	100.00	0.00	0.00	0.00	0.00
20SOZ-19	0.00	0.00	0.00	16.25	1.49	0.00	44.61	11.77	25.37	0.50	0.00	0.00
20SOZ-21	0.00	0.00	0.00	0.00	0.00	0.00	100.00	0.00	0.00	0.00	0.00	0.00
Western Privince:												
20SOZ-11	0.00	0.51	0.00	0.00	0.00	0.00	0.00	99.49	0.00	0.00	0.00	0.00
20SOZ-13	0.00	0.00	0.00	0.00	0.00	0.00	0.00	100.00	0.00	0.00	0.00	0.00
20SOZ-14	5.88	12.01	30.88	0.74	1.96	0.00	0.00	48.28	0.00	0.00	0.00	0.25
20SOZ-15	0.00	100.00	0.00	0.00	0.00	0.00	0.00	0.00	0.00	0.00	0.00	0.00
20SOZ-16	91.04	8.96	0.00	0.00	0.00	0.00	0.00	0.00	0.00	0.00	0.00	0.00

Table 2: Mapped watershed sample information:

Sample	Coordinates (WGS84):		River Drainage	Terranes Exposed in Drainage (>5% Areal Exposure)	Zircon:	
	Latitude	Longitude			Number of Analyses	Concordant Ages
Eastern Province:						
20SOZ-01	-46.276	167.730	Waiau	Takaka, Median Batholith, Caples, Dun Mountain, Brook street	82	75
20SOZ-02	-46.055	170.194	Taeri	Caples, Rakaia	90	88
20SOZ-03	-46.210	169.710	Clutha	Caples, Rakaia	96	92
20SOZ-07	-45.001	168.758	Shotover		66	33
20SOZ-08	-44.263	169.190	Makarora	Rakaia	85	65
20SOZ-19	-41.441	173.965	Wairau	Caples, Rahau, Rakaia, Kaweka	101	84
20SOZ-21	-42.416	173.633	Kowhai	Pahau	100	92
Western Privince:						
20SOZ-11	-43.859	169.051	Haast	Rakaia	64	53
20SOZ-12	-43.596	169.602	Mahitahi	Rakaia	97	86
20SOZ-13	-43.388	170.173	Waiho	Rakaia	100	72
20SOZ-14	-41.805	171.600	Buller	Takaka, Buller, Median Batholith, Rakaia	100	91
20SOZ-15	-41.859	171.945	Inangahaua	Buller	97	85
20SOZ-16	-40.987	172.820	Takaka	Takaka, buller	57	50

Table 3: Number of grains for each sample within corresponding time bins (Ma) from 2600-65 Ma.

Sample #	Late Cret. 65-100	Early Cret. 100-146	Jurassic 146-200	Trias. 200-251	Per. 251-300	Carb. 300-360	Dev-Sil. 360-444	Ord-Cam. 444-542	Precambrian 542-2600
20SOZ-01	0	32	5	1	8	17	0	0	0
20SOZ-02	0	9	8	26	26	6	4	8	4
20SOZ-03	0	0	1	31	30	12	4	10	4
20SOZ-07	0	0	6	11	7	2	3	2	2
20SOZ-08B	0	0	3	27	30	7	4	6	6
20SOZ-11B	0	0	0	20	15	3	7	6	3
20SOZ-12	0	0	0	8	13	4	3	4	3
20SOZ-13	0	0	0	30	7	5	5	8	17
20SOZ-14	0	14	0	5	11	11	17	17	16
20SOZ-15	0	11	1	1	2	5	23	5	35
20SOZ-16	0	10	1	0	0	10	3	2	31
20SOZ-19	0	6	7	11	20	8	3	7	22
20SOZ-21	0	27	10	14	15	7	7	5	7

Table 4: KS test results compared to the basement Zealandia Cordillera (500-100 Ma) data set from: Kimbrough and Tulloch, 1989; Kimbrough et al., 1994; Muir et al., 1996; Waight et al., 1997; Ireland and Gibson, 1998; Muir et al., 1998; Davids, 1999; Tulloch and Kimbrough et al., 1999; Tulloch and Kimbrough et al., 2003; Allibone and Tulloch, 2004; Gollan, 2006; Price et al., 2006; Bolhar et al., 2008; Scott and Palin. 2008; Tulloch et al., 2009; Turnbull et al., 2010; Tulloch et al., 2011, Turnbull et al., 2013; McCoy-West et al., 2014; Allibone et al., 2016; Decker, 2016; Martin et al., 2016; Schwartz et al., 2017; Van der Meer et al., 2018; Buriticá et al., 2019; and Ringwood *et al.*, 2021. Yellow highlighted cells indicate a "P" Value greater than 0.05 making the samples not statistically different i.e. derived from the same population. Green highlighted cells are the sample names.

	Plutonic Comparis	20SOZ-01	20SOZ-02	20SOZ-03	20SOZ-07	20SOZ-08B	20SOZ-11B	20SOZ-12	20SOZ-13	20SOZ-14	20SOZ-15	20SOZ-16	20SOZ-19	20SOZ-21
Plutonic Comparison		0.008	0.000	0.000	0.000	0.000	0.000	0.000	0.000	0.000	0.000	0.000	0.000	0.000
20SOZ-01	0.008		0.000	0.000	0.000	0.000	0.000	0.000	0.000	0.000	0.000	0.000	0.000	0.005
20SOZ-02	0.000	0.000		0.005	**0.810**	**0.163**	**0.230**	**0.262**	0.002	0.000	0.000	0.000	0.000	0.008
20SOZ-03	0.000	0.000	0.005		**0.143**	**0.710**	**0.759**	**0.117**	0.003	0.000	0.000	0.000	0.000	0.000
20SOZ-07	0.000	0.000	**0.810**	**0.143**		**0.507**	**0.618**	**0.930**	0.042	0.002	0.000	0.000	0.001	0.004
20SOZ-08B	0.000	0.000	**0.163**	**0.710**	**0.507**		**0.786**	**0.932**	0.009	0.000	0.000	0.000	0.000	0.000
20SOZ-11B	0.000	0.000	**0.230**	**0.759**	**0.618**	**0.786**		**0.979**	**0.091**	0.003	0.000	0.000	0.018	0.000
20SOZ-12	0.000	0.000	**0.262**	**0.117**	**0.930**	**0.932**	**0.979**		0.009	0.000	0.000	0.000	0.001	0.000
20SOZ-13	0.000	0.000	0.002	0.003	0.042	0.009	**0.091**	0.009		**0.074**	0.000	0.000	0.032	0.000
20SOZ-14	0.000	0.000	0.000	0.000	0.002	0.000	0.003	0.000	**0.074**		0.002	0.000	**0.157**	0.000
20SOZ-15	0.000	0.000	0.000	0.000	0.000	0.000	0.000	0.000	0.000	0.002		**0.419**	0.000	0.000
20SOZ-16	0.000	0.000	0.000	0.000	0.000	0.000	0.000	0.000	0.000	0.000	**0.419**		0.002	0.000
20SOZ-19	0.000	0.000	0.000	0.000	0.001	0.000	0.018	0.001	0.032	**0.157**	0.000	0.002		0.000
20SOZ-21	0.000	0.005	0.008	0.000	0.004	0.000	0.000	0.000	0.000	0.000	0.000	0.000	0.000	

Table 5: KS test results compared to the basement sandstone DZ data set from Adams (*et al.*, 2007). Yellow highlighted cells indicate a "P" Value greater than 0.05 making the samples not statistically different. Green highlighted cells are the sample names.

	Adams Accretionary comparison	20SOZ-01	20SOZ-02	20SOZ-03	20SOZ-07	20SOZ-08B	20SOZ-11B	20SOZ-12	20SOZ-13	20SOZ-14	20SOZ-15	20SOZ-16	20SOZ-19	20SOZ-21
Adams Accretionary comparison		0.000	0.001	0.018	**0.102**	0.006	0.003	0.003	0.000	0.000	0.000	0.000	0.000	0.000
20SOZ-01	0.000		0.000	0.000	0.000	0.000	0.000	0.000	0.000	0.000	0.000	0.000	0.000	0.005
20SOZ-02	0.001	0.000		0.005	**0.810**	**0.163**	**0.230**	**0.262**	0.002	0.000	0.000	0.000	0.000	0.008
20SOZ-03	0.018	0.000	0.005		**0.143**	**0.710**	**0.759**	**0.117**	0.003	0.000	0.000	0.000	0.000	0.000
20SOZ-07	**0.102**	0.000	**0.810**	**0.143**		**0.507**	**0.618**	**0.930**	0.042	0.002	0.000	0.000	0.001	0.004
20SOZ-08B	0.006	0.000	**0.163**	**0.710**	**0.507**		**0.786**	**0.932**	0.009	0.000	0.000	0.000	0.000	0.000
20SOZ-11B	0.003	0.000	**0.230**	**0.759**	**0.618**	**0.786**		**0.979**	**0.091**	0.003	0.000	0.000	0.018	0.000
20SOZ-12	0.003	0.000	**0.262**	**0.117**	**0.930**	**0.932**	**0.979**		0.009	0.000	0.000	0.000	0.001	0.000
20SOZ-13	0.000	0.000	0.002	0.003	0.042	0.009	**0.091**	0.009		**0.074**	0.000	0.000	0.032	0.000
20SOZ-14	0.000	0.000	0.000	0.000	0.002	0.000	0.003	0.000	**0.074**		0.002	0.000	**0.157**	0.000
20SOZ-15	0.000	0.000	0.000	0.000	0.000	0.000	0.000	0.000	0.000	0.002		**0.419**	0.000	0.000
20SOZ-16	0.000	0.000	0.000	0.000	0.000	0.000	0.000	0.000	0.000	0.000	**0.419**		0.002	0.000
20SOZ-19	0.000	0.000	0.000	0.000	0.001	0.000	0.018	0.001	0.032	**0.157**	0.000	0.002		0.000
20SOZ-21	0.000	0.005	0.008	0.000	0.004	0.000	0.000	0.000	0.000	0.000	0.000	0.000	0.000	

Table 6: Table **6A:** Individual KS tests between the Adams (*et al.*, 2015) and Buller terrane U/Pb detrital zircon grain-age compilation and 20SOZ-15. Table **6B**: Individual KS tests between Adams (*et al.*, 2007) Caples terrane U/Pb detrital zircon grain-age compilation and samples 20SOZ-01, 02, and 03. Yellow highlighted cells indicate a "P" Value greater than 0.05 making the samples not statistically different. Green highlighted cells are the sample names.

Table 6A:	Adams Caples Terrane	20SOZ-01	20SOZ-02	20SOZ-03
Adams Caples Terrane		0.000	0.000	0.000
20SOZ-01	0.000		0.000	0.000
20SOZ-02	0.000	0.000		0.001
20SOZ-03	0.000	0.000	0.001	

Table 6B:	Adams_Buller_ Compilation N= 800	20SOZ-15
Adams_Buller_Compilation		0.000
20SOZ-15	0.000	

Table 7: Likeness test results compared to the basement sandstone DZ data set from Adams (*et al.*, 2017). Yellow cells indicate a greater than 50% Likeness to the bedrock.

Likeness Test Comparison:	20SOZ-01	20SOZ-02	20SOZ-03	20SOZ-07	20SOZ-08B	20SOZ-11B	20SOZ-12	20SOZ-13	20SOZ-14	20SOZ-15	20SOZ-16	20SOZ-19	20SOZ-21
DZ Comparison	41.9%	30.4%	25.8%	23.3%	22.9%	23.7%	23.2%	21.1%	52.9%	32.7%	54.6%	30.2%	37.7%

Table 8: Cross-Correlation Coefficient for 13 Samples data compared to Bedrock Central Arc and Accretionary Complex grain-age compilations: Adams *et al*., 2015; Campbell *et al*., 2020 (forearc); Campbell, Rosenbaum, *et al*., 2020 (Murihihuki terrane); Campbell, Rosenbaum, Allen, and Mortimer, 2020, and Adams (*et al*., 2015). Orange Highlighted cells indicate a sample has greater than > 0.5 R^2 Cross-correlation compared to the grain-age compilation.

Cross Correlation Coefficient	20SOZ-01	20SOZ-02	20SOZ-03	20SOZ-07	20SOZ-08B	20SOZ-11B	20SOZ-12	20SOZ-13	20SOZ-14	20SOZ-15	20SOZ-16	20SOZ-19	20SOZ-21	Adams 2015 Buller & Takaka	Adams Accretionary comparison	Campbell_2020_Forarc_terranes: Dunmountain,	2020_campbell_Murhihiku_terrane_gondwanna	2020_Campbell_Zircon_Petrochronology_Zealandia
20SOZ-01	1.000	0.024	0.009	0.013	0.003	0.008	0.010	0.015	0.358	0.086	0.310	0.004	0.297	0.059	0.005	0.005	0.006	0.005
20SOZ-02	0.024	1.000	0.625	0.585	0.721	0.571	0.645	0.443	0.118	0.023	0.000	0.320	0.424	0.052	0.497	0.615	0.573	0.615
20SOZ-03	0.009	0.625	1.000	0.667	0.761	0.694	0.692	0.482	0.112	0.050	0.005	0.387	0.254	0.023	0.831	0.922	0.637	0.922
20SOZ-07	0.013	0.585	0.667	1.000	0.630	0.639	0.740	0.610	0.029	0.074	0.013	0.237	0.184	0.059	0.570	0.561	0.828	0.561
20SOZ-08B	0.003	0.721	0.761	0.630	1.000	0.793	0.811	0.565	0.073	0.074	0.026	0.603	0.190	0.041	0.573	0.781	0.662	0.781
20SOZ-11B	0.008	0.571	0.694	0.639	0.793	1.000	0.801	0.619	0.061	0.025	0.022	0.390	0.174	0.041	0.504	0.653	0.727	0.653
20SOZ-12	0.010	0.645	0.692	0.740	0.811	0.801	1.000	0.657	0.046	0.059	0.010	0.376	0.163	0.062	0.507	0.580	0.763	0.580
20SOZ-13	0.015	0.443	0.482	0.610	0.565	0.619	0.657	1.000	0.026	0.042	0.034	0.170	0.080	0.007	0.386	0.405	0.684	0.405
20SOZ-14	0.358	0.118	0.112	0.029	0.073	0.061	0.046	0.026	1.000	0.094	0.362	0.032	0.193	0.002	0.090	0.092	0.009	0.092
20SOZ-15	0.086	0.023	0.050	0.074	0.074	0.025	0.059	0.042	0.094	1.000	0.025	0.050	0.058	0.011	0.041	0.043	0.099	0.043
20SOZ-16	0.310	0.000	0.005	0.013	0.026	0.022	0.010	0.034	0.362	0.025	1.000	0.011	0.058	0.001	0.007	0.026	0.044	0.026
20SOZ-19	0.004	0.320	0.387	0.237	0.603	0.390	0.376	0.170	0.032	0.050	0.011	1.000	0.067	0.018	0.299	0.428	0.260	0.428
20SOZ-21	0.297	0.424	0.254	0.184	0.190	0.174	0.163	0.080	0.193	0.058	0.058	0.067	1.000	0.081	0.209	0.254	0.182	0.254
Adams 2015 Buller & Takaka	0.059	0.052	0.023	0.059	0.041	0.041	0.062	0.007	0.002	0.011	0.001	0.018	0.081	1.000	0.026	0.031	0.067	0.031
dams Accretionary compariso	0.005	0.497	0.831	0.570	0.573	0.504	0.507	0.386	0.090	0.041	0.007	0.299	0.209	0.026	1.000	0.825	0.556	0.825
arc_terranes: Dunmountain, Ka	0.005	0.615	0.922	0.561	0.781	0.653	0.580	0.405	0.092	0.043	0.026	0.428	0.254	0.031	0.825	1.000	0.595	1.000
mpbell_Murhihiku_terrane_gor	0.006	0.573	0.637	0.828	0.662	0.727	0.763	0.684	0.009	0.099	0.044	0.260	0.182	0.067	0.556	0.595	1.000	0.595
pbell_Zircon_Petrochronology_	0.005	0.615	0.922	0.561	0.781	0.653	0.580	0.405	0.092	0.043	0.026	0.428	0.254	0.031	0.825	1.000	0.595	1.000

Table 9: Likeness test for 13 Samples data compared to Bedrock Central Arc and Accretionary Complex grain-age compilations: Adams *et al*., 2015; Campbell *et al*., 2020 (forearc); Campbell, Rosenbaum, *et al*., 2020 (Murihihuki terrane); Campbell, Rosenbaum, Allen, and Mortimer, 2020, and Adams (*et al*., 2015). Blue Highlighted cells indicate a sample has greater than > 0.5 R^2 Cross-correlation compared to the grain-age compilation.

Likeness value	20SOZ-01	20SOZ-02	20SOZ-03	20SOZ-07	20SOZ-08B	20SOZ-11B	20SOZ-12	20SOZ-13	20SOZ-14	20SOZ-15	20SOZ-16	20SOZ-19	20SOZ-21	Adams 2015 Buller & Takaka	Adams Accretionary comparison	Campbell_2020_Forarc_terranes: Dunmountain,	2020_campbell_Murhihiku_terrane_gondwanna	2020_Campbell_Zircon_Petrochronology_Zealandia
20SOZ-01	1.000	0.299	0.176	0.177	0.244	0.181	0.209	0.217	0.406	0.360	0.455	0.397	0.444	0.250	0.148	0.114	0.172	0.114
20SOZ-02	0.299	1.000	0.680	0.695	0.782	0.663	0.730	0.631	0.479	0.371	0.404	0.576	0.623	0.346	0.559	0.513	0.619	0.513
20SOZ-03	0.176	0.680	1.000	0.717	0.719	0.685	0.721	0.629	0.484	0.334	0.394	0.565	0.535	0.364	0.752	0.689	0.605	0.689
20SOZ-07	0.177	0.695	0.717	1.000	0.681	0.688	0.755	0.655	0.436	0.323	0.355	0.539	0.554	0.326	0.615	0.512	0.734	0.512
20SOZ-08B	0.244	0.782	0.719	0.681	1.000	0.770	0.789	0.700	0.465	0.348	0.361	0.685	0.533	0.369	0.593	0.614	0.632	0.614
20SOZ-11B	0.181	0.663	0.685	0.688	0.770	1.000	0.794	0.718	0.524	0.434	0.353	0.615	0.547	0.390	0.527	0.537	0.605	0.537
20SOZ-12	0.209	0.730	0.721	0.755	0.789	0.794	1.000	0.717	0.485	0.381	0.387	0.615	0.573	0.347	0.584	0.506	0.684	0.506
20SOZ-13	0.217	0.631	0.629	0.655	0.700	0.718	0.717	1.000	0.550	0.460	0.391	0.636	0.511	0.487	0.521	0.459	0.608	0.459
20SOZ-14	0.406	0.479	0.484	0.436	0.465	0.524	0.485	0.550	1.000	0.605	0.653	0.591	0.541	0.524	0.357	0.256	0.259	0.256
20SOZ-15	0.360	0.371	0.334	0.323	0.348	0.434	0.381	0.460	0.605	1.000	0.602	0.515	0.486	0.580	0.248	0.190	0.199	0.190
20SOZ-16	0.455	0.404	0.394	0.355	0.361	0.353	0.387	0.391	0.653	0.602	1.000	0.522	0.474	0.612	0.306	0.202	0.219	0.202
20SOZ-19	0.397	0.576	0.565	0.539	0.685	0.615	0.615	0.636	0.591	0.515	0.522	1.000	0.546	0.527	0.464	0.418	0.446	0.418
20SOZ-21	0.444	0.623	0.535	0.554	0.533	0.547	0.573	0.511	0.541	0.486	0.474	0.546	1.000	0.335	0.436	0.362	0.442	0.362
Adams 2015 Buller & Takaka	0.250	0.346	0.364	0.326	0.369	0.390	0.347	0.487	0.524	0.580	0.612	0.527	0.335	1.000	0.268	0.245	0.239	0.245
dams Accretionary compariso	0.148	0.559	0.752	0.615	0.593	0.527	0.584	0.521	0.357	0.248	0.306	0.464	0.436	0.268	1.000	0.726	0.580	0.726
arc_terranes: Dunmountain, Ka	0.114	0.513	0.689	0.512	0.614	0.537	0.506	0.459	0.256	0.190	0.202	0.418	0.362	0.245	0.726	1.000	0.597	1.000
mpbell_Murhihiku_terrane_gor	0.172	0.619	0.605	0.734	0.632	0.605	0.684	0.608	0.259	0.199	0.219	0.446	0.442	0.239	0.580	0.597	1.000	0.597
pbell_Zircon_Petrochronology_	0.114	0.513	0.689	0.512	0.614	0.537	0.506	0.459	0.256	0.190	0.202	0.418	0.362	0.245	0.726	1.000	0.597	1.000

Table 10: Cross-correlation coefficient for 13 samples compared against the Plutonic Bedrock Compilation ((Kimbrough and Tulloch, 1989; Kimbrough et al., 1994; Muir et al., 1996; Waight et al., 1997; Ireland and Gibson, 1998; Muir et al., 1998; Davids, 1999; Tulloch and Kimbrough et al., 1999; Tulloch and Kimbrough et al., 2003; Allibone and Tulloch, 2004; Gollan, 2006; Price et al., 2006; Bolhar et al., 2008; Scott and Palin. 2008; Tulloch et al., 2009; Turnbull et al., 2010; Tulloch et al., 2011, Turnbull et al., 2013; McCoy-West et al., 2014; Allibone et al., 2016; Decker, 2016; Martin et al., 2016; Schwartz et al., 2017; Van der Meer et al., 2018; Buriticá et al., 2019; Ringwood *et al.*, 2021). Orange highlighted cells indicate a > 0.5 R^2 value.

Cross Correlation Coefficient	20SOZ-01	20SOZ-02	20SOZ-03	20SOZ-07	20SOZ-08B	20SOZ-11B	20SOZ-12	20SOZ-13	20SOZ-14	20SOZ-15	20SOZ-16	20SOZ-19	20SOZ-21	Plutonic Compilation
20SOZ-01	1	0.08044	0.002044853	0.001769528	0.010251763	0.007871238	0.005432	0.001699	0.425345805	0.170586	0.348535281	0.057140614	0.374417156	0.64062807
20SOZ-02	0.080440448	1	0.676759525	0.65170148	0.773286089	0.655109901	0.712899	0.525627	0.260954574	0.025621	0.037243562	0.446893273	0.53131261	0.13383361
20SOZ-03	0.002044853	0.67676	1	0.708666487	0.792903333	0.733722383	0.732161	0.542001	0.219522291	0.002825	0.009153141	0.462474001	0.34919093	0.01369792
20SOZ-07	0.001769528	0.651701	0.708666487	1	0.687017294	0.697118739	0.778054	0.659086	0.134504872	0.002024	0.007415852	0.355840394	0.29550432	0.0172715
20SOZ-08B	0.010251763	0.773286	0.792903333	0.687017294	1	0.832824182	0.846525	0.627441	0.203062189	0.004328	0.002747828	0.667792625	0.310259119	0.00964951
20SOZ-11B	0.007871238	0.65511	0.733722383	0.697118739	0.832824182	1	0.841422	0.676272	0.205194531	0.029723	0.006846119	0.517069403	0.307615029	0.01080916
20SOZ-12	0.005432452	0.712899	0.732160658	0.778053774	0.846524951	0.841421932	1	0.706743	0.178268992	0.011916	0.012390933	0.502177869	0.291959822	0.01655467
20SOZ-13	0.001698557	0.525627	0.542001007	0.659086152	0.627441025	0.676272036	0.706743	1	0.133071987	0.011126	0.001428807	0.30440539	0.183612805	0.00927255
20SOZ-14	0.425345805	0.260955	0.219522291	0.134504872	0.203062189	0.205194531	0.178269	0.133072	1	0.284582	0.454071681	0.202054192	0.352042794	0.24753276
20SOZ-15	0.170585806	0.025621	0.002824957	0.002023979	0.004327742	0.029722523	0.011916	0.011126	0.284581533	1	0.135252469	0.04116951	0.202780662	0.23327295
20SOZ-16	0.348535281	0.037244	0.009153141	0.007415852	0.002747828	0.006846119	0.012391	0.001429	0.454071681	0.135252	1	0.033481669	0.144906159	0.22641228
20SOZ-19	0.057140614	0.446893	0.462474001	0.355840394	0.667792625	0.517069403	0.502178	0.304405	0.202054192	0.04117	0.033481669	1	0.213043207	0.0116531
20SOZ-21	0.374417156	0.531313	0.34919093	0.29550432	0.310259119	0.307615029	0.29196	0.183613	0.352042794	0.202781	0.144906159	0.213043207	1	0.64246635
Plutonic compilation	0.640628075	0.133834	0.013697917	0.017271501	0.009649513	0.010809161	0.016555	0.009273	0.24753276	0.233273	0.226412275	0.011653103	0.642466353	1

Appendix A

U-Pb Standard data for Temora-2 geochronologic standard. N – 150 Concordant grains in black. Red grain ages indicate > 10% discordance.

207/235 age Ma	1 sigma abs err Ma	206/238 age Ma	1 sigma abs err Ma	207/206 age Ma	1 sigma abs err Ma	Best age age† Ma	207/236 age Ma
436.5	8.5	432.2	8.7	459.0	53.0	431.9	276.0
433.7	8.3	454.0	10.0	328.0	47.0	456.0	250.8
435.8	8.3	453.2	9.4	345.0	44.0	454.7	252.9
418.5	8.5	412.6	7.4	451.0	48.0	412.1	265.2
440.2	8.4	439.6	8.4	443.0	50.0	439.5	273.4
400.0	12.0	397.0	11.0	415.0	65.0	397.0	258.9
394.9	7.0	408.7	7.3	315.0	54.0	409.8	234.5
414.8	5.5	434.6	7.6	306.0	35.0	436.2	233.5
419.5	5.9	437.2	6.1	323.0	41.0	438.7	240.7
405.9	7.9	389.2	6.8	502.0	54.0	387.8	272.0
408.3	4.2	399.3	5.7	459.0	30.0	398.6	255.3
394.7	7.3	393.9	7.0	399.0	45.0	393.9	245.6
427.3	8.3	432.5	7.8	399.0	43.0	433.0	257.7
384.1	6.9	398.3	8.2	299.0	53.0	399.4	226.8
400.6	7.3	389.2	7.3	467.0	49.0	388.2	261.8
402.3	6.6	417.7	8.4	315.0	50.0	418.9	236.1
415.0	9.0	398.8	6.7	506.0	52.0	397.5	275.1
419.0	8.8	413.9	9.8	447.0	50.0	413.5	265.9
432.1	7.9	433.7	7.9	423.0	34.0	433.8	259.9
401.7	7.7	391.0	7.2	463.0	49.0	390.2	261.4
419.6	8.2	427.9	9.4	374.0	37.0	428.6	247.9
425.1	6.3	434.6	7.5	374.0	40.0	435.3	251.5
439.8	6.2	448.5	8.1	395.0	39.0	449.2	260.9
415.5	6.0	388.2	5.6	570.0	48.0	386.0	285.2
450.2	8.0	453.8	9.7	431.0	46.0	454.1	274.0
468.3	7.2	476.7	9.5	427.0	38.0	477.4	277.6
434.1	8.2	442.3	9.3	391.0	31.0	443.0	254.3
429.1	8.2	444.1	8.7	349.0	49.0	445.4	252.7
429.0	7.4	419.0	8.2	483.0	58.0	418.2	279.4
419.0	10.0	405.3	8.0	498.0	60.0	404.2	279.0
427.4	9.1	438.1	9.7	370.0	38.0	439.0	250.8
421.2	7.1	402.5	7.9	525.0	38.0	401.0	275.2

405.5	8.4	388.7	8.1	502.0	56.0	387.3	272.8
412.4	8.8	408.2	8.4	436.0	52.0	407.9	262.1
410.1	8.7	412.0	10.0	399.0	55.0	412.0	256.0
389.5	8.6	393.4	8.2	366.0	54.0	393.8	241.4
411.0	11.0	392.5	6.9	517.0	76.0	391.0	285.7
392.0	11.0	386.4	8.8	427.0	60.0	385.9	255.9
406.5	7.9	389.2	8.3	506.0	57.0	387.8	274.5
429.0	10.0	431.4	6.9	419.0	57.0	431.5	267.7
415.0	11.0	404.6	9.8	471.0	71.0	403.7	276.9
415.0	11.0	414.7	7.7	415.0	69.0	414.7	266.1
411.0	9.4	408.1	7.4	427.0	52.0	407.9	259.7
426.1	8.1	409.4	7.7	517.0	59.0	408.1	284.4
414.5	9.6	408.7	6.5	447.0	58.0	408.2	267.0
358.4	7.6	345.4	6.3	443.0	60.0	344.4	246.5
365.0	12.0	372.9	8.7	315.0	80.0	373.6	233.0
439.4	6.7	442.9	7.3	421.0	43.0	443.2	266.5
433.0	8.4	439.6	9.1	398.0	33.0	440.1	255.7
415.0	10.0	404.1	9.1	473.0	43.0	403.3	265.3
423.4	6.7	416.2	8.1	463.0	42.0	415.6	267.0
437.9	7.3	437.5	7.0	440.0	37.0	437.5	266.4
425.3	5.9	429.0	5.4	405.0	42.0	429.4	257.5
419.0	6.7	433.3	8.6	341.0	37.0	434.4	242.1
415.0	6.8	424.0	6.8	365.0	33.0	424.7	242.5
413.2	7.9	418.3	6.1	385.0	40.0	418.6	248.0
417.3	8.2	427.7	8.1	360.0	37.0	428.6	244.4
421.7	4.4	430.0	5.7	377.0	32.0	430.7	247.2
426.6	7.5	420.3	6.6	461.0	49.0	419.8	270.6
407.8	6.4	408.4	6.5	404.0	32.0	408.5	246.1
426.4	8.4	421.1	6.1	455.0	52.0	420.7	270.5
418.3	9.0	412.4	6.4	451.0	52.0	412.0	266.7
418.4	7.5	423.5	7.0	390.0	34.0	423.9	248.6
404.0	7.4	403.0	6.7	410.0	45.0	402.9	251.1
430.9	9.9	423.3	9.0	472.0	57.0	422.7	277.6
446.2	6.3	449.8	7.8	428.0	34.0	450.1	266.8
391.0	6.4	396.0	7.8	362.0	46.0	396.4	238.1
402.2	5.9	399.4	8.3	418.0	53.0	399.1	255.6
421.0	9.5	424.6	7.1	401.0	55.0	424.9	260.3
407.6	7.4	398.8	7.7	458.0	62.0	398.1	268.5
435.2	7.5	453.5	8.2	340.0	38.0	455.0	249.2
421.9	8.8	412.5	7.3	474.0	53.0	411.8	272.7

398.5	7.9	386.0	8.0	471.0	41.0	385.1	258.4
407.8	8.0	391.5	5.2	501.0	57.0	390.2	273.6
596.0	22.0	580.0	31.0	654.0	114.0	579.0	397.6
319.0	13.0	323.0	12.0	295.0	85.0	323.0	214.0
637.0	16.0	658.0	16.0	564.0	66.0	660.0	384.6
388.0	15.0	388.0	14.0	393.0	84.0	387.0	258.4
734.0	17.0	726.0	17.0	756.0	65.0	726.0	449.0
162.1	4.4	156.6	3.5	243.0	68.0	156.3	141.4
401.7	6.9	404.5	9.1	386.0	31.0	404.7	240.4
374.9	6.3	382.4	7.1	329.0	33.0	383.0	220.0
1067.0	26.0	1075.0	32.0	1052.0	64.0	1076.0	638.9
1268.0	17.0	1267.0	25.0	1268.0	33.0	1267.0	739.3
1227.0	18.0	1280.0	30.0	1136.0	32.0	1288.0	725.4
333.5	8.0	318.1	9.3	442.0	50.0	316.9	233.7
434.0	5.9	435.2	6.2	428.0	32.0	435.2	260.7
424.3	6.2	428.9	9.5	400.0	37.0	429.3	254.7
430.2	7.7	415.5	8.2	510.0	32.0	414.3	273.3
412.4	8.3	408.3	8.8	436.0	34.0	408.0	254.5
427.8	8.4	436.3	9.7	382.0	38.0	437.1	253.2
418.5	8.2	414.8	7.7	439.0	42.0	414.5	260.6
422.4	8.3	415.2	9.1	462.0	37.0	414.7	264.3
416.1	6.9	400.5	7.2	503.0	38.0	399.3	269.3
415.2	8.1	403.9	9.4	479.0	36.0	402.9	264.1
422.9	7.9	410.6	7.6	490.0	36.0	409.6	268.6
415.6	7.7	410.4	7.8	444.0	29.0	410.0	254.8
417.0	8.1	421.0	11.0	397.0	43.0	421.0	253.7
422.5	6.8	414.8	8.0	465.0	40.0	414.2	266.1
414.9	6.3	417.1	7.9	403.0	42.0	417.2	253.2
408.6	6.2	401.8	8.3	447.0	29.0	401.3	253.0
406.3	6.0	411.3	8.0	378.0	31.0	411.7	240.7
403.2	7.3	401.9	9.3	411.0	32.0	401.8	245.8
417.6	6.7	423.1	7.8	388.0	34.0	423.5	248.3
417.5	6.9	414.1	8.8	436.0	27.0	413.8	253.6
412.0	5.5	406.4	6.5	444.0	24.0	406.0	251.6
412.7	8.0	412.5	8.6	414.0	33.0	412.5	250.3
416.4	7.3	421.0	7.6	391.0	38.0	421.4	249.9
439.4	6.1	419.0	7.6	547.0	32.0	417.4	283.2
425.1	7.3	416.0	7.5	475.0	36.0	415.2	267.0
427.7	6.5	414.6	7.0	499.0	39.0	413.5	273.4
429.0	7.8	422.0	9.0	467.0	28.0	421.4	263.8

414.8	6.3	408.9	8.1	448.0	31.0	408.4	256.4
420.5	6.1	422.6	8.9	409.0	38.0	422.7	254.9
422.9	7.1	420.1	8.3	438.0	52.0	419.9	266.7
426.5	6.0	425.8	9.7	430.0	35.0	425.8	259.8
413.7	6.7	419.6	6.3	381.0	37.0	420.1	246.5
422.4	6.4	427.3	5.6	396.0	37.0	427.7	252.6
415.6	5.9	415.8	7.5	414.0	27.0	415.8	248.9
425.0	11.0	422.6	8.8	437.0	54.0	422.5	267.7
420.1	5.1	420.1	6.9	420.0	31.0	420.0	253.5
416.1	7.5	418.9	9.1	400.0	28.0	419.1	247.1
429.2	7.2	413.9	7.0	512.0	32.0	412.7	273.2
446.4	15.0	451.7	11.2	383.4	62.2	450.3	265.4
435.3	13.2	440.9	16.6	375.8	54.9	436.7	256.6
410.6	14.9	394.8	11.6	517.1	99.9	390.9	296.2
394.6	21.0	376.4	11.8	495.1	96.4	372.6	281.6
394.1	14.3	390.6	14.3	402.7	75.6	385.9	255.4
420.9	13.4	429.4	13.7	404.4	76.3	425.8	271.3
406.7	16.6	406.9	13.7	430.2	93.4	403.3	276.8
429.2	13.9	410.1	12.9	510.4	79.6	405.9	289.1
403.4	18.6	392.1	13.1	524.6	127.5	387.3	309.8
488.3	30.3	492.4	20.6	568.5	133.7	491.6	359.8
474.9	28.0	454.6	20.4	659.8	147.0	451.2	372.6
426.5	20.4	429.7	17.6	524.5	95.1	424.2	310.8
456.1	24.0	474.2	19.2	467.9	125.3	469.1	324.5
452.4	16.2	470.4	14.8	397.4	110.4	468.0	298.8
442.1	15.7	435.9	16.8	499.9	75.8	430.3	295.0
443.1	16.6	456.4	15.9	437.1	86.6	452.5	293.9
432.0	27.9	446.6	21.2	607.1	153.6	439.2	365.9
433.2	11.4	429.3	13.2	501.0	61.7	425.6	289.3
415.7	23.2	399.3	18.8	544.3	130.5	390.9	315.4
474.8	20.4	499.3	21.7	435.3	97.6	493.0	312.5
461.7	19.0	483.4	17.0	455.7	60.8	480.1	298.4
422.4	20.5	411.1	20.5	512.5	107.5	402.0	301.5
421.3	16.7	426.2	14.2	477.4	101.3	422.6	300.6
413.5	24.1	406.9	22.4	607.6	123.4	396.0	334.4
432.1	12.7	449.5	14.0	397.6	84.4	446.7	281.7
404.3	16.9	405.1	10.2	450.8	110.9	403.1	290.2
414.2	22.0	415.8	18.6	508.2	124.2	408.8	313.2
622.7	68.9	486.2	14.3	1119.3	251.4	473.8	512.6

410.4	6.9	390.3	6.7	525.0	53.0	388.7	277.5
413.7	8.4	390.1	7.7	548.0	52.0	388.2	282.4
448.3	6.1	454.8	7.5	415.0	47.0	455.3	271.0
441.7	7.5	442.9	9.1	435.0	40.0	443.0	268.6
422.0	10.0	397.6	8.7	559.0	65.0	395.6	292.9
392.0	10.0	372.5	8.3	506.0	71.0	371.0	274.8
417.8	8.1	395.4	6.8	544.0	56.0	393.5	284.7
421.0	12.0	400.0	9.8	540.0	62.0	398.3	287.9
365.4	9.5	345.4	8.9	494.0	73.0	343.8	264.4
379.0	10.0	360.8	6.6	491.0	64.0	359.4	264.3
425.3	6.6	404.5	6.5	539.0	49.0	402.8	283.6
424.0	13.0	398.9	7.4	564.0	64.0	397.4	293.7
657.0	25.0	623.0	32.0	778.0	107.0	619.0	435.1
138.3	6.4	128.7	4.6	306.0	99.0	128.1	163.3
2900.0	30.0	2333.0	57.0	3321.0	27.0	3321.0	2033.4
466.0	20.0	439.0	13.0	603.0	77.0	437.0	320.9
440.7	9.4	406.9	6.9	621.0	43.0	404.1	300.5
399.5	9.0	376.0	12.0	539.0	59.0	374.0	279.3
2081.0	23.0	1667.0	40.0	2520.0	29.0	2520.0	1580.3
2446.0	32.0	2247.0	59.0	2616.0	32.0	2616.0	1561.0
429.0	17.0	407.7	10.1	497.0	82.6	404.6	285.0
432.0	18.7	389.6	13.3	661.3	115.8	382.8	333.1
458.2	30.6	425.2	19.1	664.0	122.7	415.8	347.4

Appendix B

U-Pb data for 11 Samples 20SOZ-01, 02, 03, 07B, 08B, 11, 12, 13, 14, 15, 16, 19, and 21. Red Grain-age information represent discordant ages that were not included in statistical analysis.

238U 206Pb	2 sigma abs	207Pb 206Pb	2 sigma	207Pb/206Pb v 238U/206Pb error corr
20SOZ-01				
54.3795	2.0318	0.0474	0.0032	0.2881
19.4494	0.6669	0.0519	0.0015	0.4998
19.2415	0.8324	0.0536	0.0147	0.2237
18.6036	0.6981	0.0540	0.0014	0.1382
19.1277	0.7435	0.0537	0.0020	0.3656
19.6883	1.1359	0.0543	0.0022	0.3422
21.7742	0.6538	0.0529	0.0018	-0.1793
46.3346	1.5237	0.0491	0.0022	0.5290
19.3169	0.5299	0.0536	0.0019	0.3665
19.7967	0.8127	0.0544	0.0019	-0.1461
20.1579	1.0951	0.0533	0.0022	0.0772
18.5252	0.6170	0.0522	0.0015	0.1533
52.7778	2.1650	0.0506	0.0034	0.3864
57.0613	2.1472	0.0487	0.0017	0.3620
56.6410	2.4572	0.0502	0.0034	0.3837
60.8604	2.0357	0.0486	0.0017	0.3018
22.8457	0.7285	0.0521	0.0017	0.5193
33.7619	1.3371	0.0500	0.0021	0.3991
19.8897	0.7225	0.0521	0.0020	0.1894
53.1748	2.1200	0.0499	0.0070	0.0903
21.1126	0.5784	0.0526	0.0017	0.1463
18.9672	0.8277	0.0542	0.0014	0.3332
53.2559	2.1317	0.0489	0.0034	0.2224
53.4881	2.3845	0.0490	0.0026	0.1405
51.8407	2.2533	0.0488	0.0022	0.6005
53.2693	2.0107	0.0491	0.0032	0.4785
19.2955	0.7820	0.0536	0.0022	0.3499
22.5482	0.7872	0.0533	0.0017	0.4169
19.8525	0.8863	0.0533	0.0016	0.5724
18.7298	0.6908	0.0537	0.0016	0.4554

21.4749	0.6671	0.0530	0.0015	0.5257
58.4193	1.8326	0.0459	0.0027	0.1234
21.7987	0.7771	0.0516	0.0018	0.3154
56.2567	2.3484	0.0505	0.0016	0.5715
49.3378	1.7052	0.0486	0.0059	0.0305
20.1975	0.8367	0.0511	0.0019	0.4240
19.1685	0.5713	0.0544	0.0018	0.1132
21.5620	0.7686	0.0519	0.0036	0.2462
56.3074	2.1172	0.0489	0.0023	0.4226
56.3705	2.1348	0.0437	0.0025	0.1849
51.8307	1.6445	0.0492	0.0038	0.1261
58.2943	1.9518	0.0486	0.0040	0.3290
58.2031	1.7001	0.0464	0.0026	0.2092
51.5819	2.6854	0.0493	0.0026	0.3658
55.9150	1.8488	0.0506	0.0030	0.1459
33.4060	1.0003	0.0507	0.0026	0.1906
53.1461	2.5678	0.0478	0.0021	0.0691
48.9066	1.8741	0.0503	0.0022	0.4783
53.9584	2.0456	0.0470	0.0023	0.4833
60.4887	2.5459	0.0467	0.0052	0.1992
52.9433	1.6042	0.0496	0.0022	-0.1167
58.9187	1.9367	0.0451	0.0056	0.0852
42.0629	4.6374	0.0506	0.0030	0.0150
52.2447	1.5632	0.0491	0.0018	-0.0409
43.6373	1.8288	0.0453	0.0048	0.2348
20.3710	0.5391	0.0533	0.0024	0.5766
51.8703	2.5510	0.0500	0.0013	0.2404
39.9935	5.0380	0.0507	0.0023	0.0016
54.2921	1.6800	0.0508	0.0021	0.4969
21.1213	0.5634	0.0528	0.0019	0.3142
50.9159	2.1891	0.0528	0.0057	0.0047
49.5208	1.7734	0.0512	0.0062	-0.2701
45.8140	1.5350	0.0515	0.0022	0.2378
30.2171	1.1357	0.0532	0.0021	0.2283
47.7990	1.7669	0.0515	0.0027	0.6850
29.9281	1.3833	0.0556	0.0034	0.4229
22.2387	0.7295	0.0554	0.0018	0.3632
43.6189	1.4734	0.0530	0.0055	0.2155
58.3846	2.6183	0.0522	0.0037	0.1894
57.3100	3.0958	0.0528	0.0030	0.1026

65.7616	1.9271	0.0519	0.0015	0.2201
57.0400	2.1521	0.0528	0.0036	0.1329
38.2803	1.5220	0.0523	0.0024	0.3173
42.3883	2.1169	0.0527	0.0043	-0.3368
10.5167	0.5295	0.0641	0.0023	0.6537
2.6381	0.0969	0.1433	0.0029	0.1514
49.7708	2.0872	0.0536	0.0067	0.1241
430.0000	12.0000	0.0541	0.0038	0.0749
468.0000	11.0000	0.0580	0.0029	-0.0372
20SOZ-02				
22.9869	0.9158	0.0537	0.0014	0.5559
11.5320	0.4214	0.0580	0.0015	0.4467
13.2382	0.4771	0.0590	0.0018	0.6538
25.5112	1.0461	0.0506	0.0022	0.4285
50.1400	1.6716	0.0500	0.0025	0.2801
50.6322	2.6072	0.0500	0.0032	0.4487
22.1732	1.0050	0.0513	0.0026	0.2948
24.8115	1.1083	0.0527	0.0018	0.4228
23.4705	0.8049	0.0524	0.0014	0.3540
17.8809	0.8406	0.0563	0.0020	0.4902
52.0015	2.2286	0.0520	0.0031	0.6064
4.7222	0.1706	0.0804	0.0039	0.4026
23.6503	0.7183	0.0517	0.0027	0.3994
12.2694	0.5746	0.0571	0.0015	0.6164
23.8906	1.0370	0.0534	0.0034	0.4007
50.8544	2.0400	0.0495	0.0042	0.5004
22.7739	0.8858	0.0509	0.0014	0.1398
28.6745	1.0712	0.0485	0.0018	0.5921
24.4230	0.9146	0.0511	0.0019	0.1752
11.9963	0.4412	0.0577	0.0031	0.3506
23.7681	1.0795	0.0522	0.0017	0.2010
34.4526	1.3066	0.0499	0.0016	0.0468
16.6932	0.6314	0.0526	0.0019	0.4050
11.3765	0.5052	0.0598	0.0017	0.3080
24.8016	1.1185	0.0529	0.0013	0.3777
30.6414	1.1967	0.0509	0.0022	0.2095
23.4027	0.8336	0.0514	0.0015	0.2085
12.4220	0.5540	0.0589	0.0016	0.2521
18.2533	0.5510	0.0524	0.0015	0.2849

25.8289	0.9632	0.0523	0.0015	0.2165
49.6364	1.6827	0.0508	0.0040	-0.2190
28.7342	0.9464	0.0504	0.0013	0.1894
28.9681	0.8316	0.0520	0.0025	0.1415
28.3285	1.0927	0.0490	0.0024	0.5094
27.6971	0.9495	0.0491	0.0026	0.2670
28.7468	1.1328	0.0506	0.0018	0.3901
23.3144	0.8713	0.0515	0.0022	0.4886
31.7259	0.8377	0.0500	0.0013	0.1001
23.9822	0.8253	0.0495	0.0026	0.1778
33.0399	1.0127	0.0488	0.0012	-0.1349
24.2077	0.8126	0.0515	0.0014	0.4563
7.7233	0.3520	0.0667	0.0023	0.1438
27.1377	0.9409	0.0518	0.0013	0.0940
29.0354	1.0156	0.0519	0.0016	0.4520
23.6811	0.7860	0.0510	0.0016	0.4795
26.4146	0.9257	0.0539	0.0011	0.0534
23.5158	0.8580	0.0514	0.0024	0.2957
25.5194	1.0112	0.0521	0.0020	0.0967
24.9809	0.9943	0.0498	0.0016	0.2962
19.3841	0.6285	0.0554	0.0023	0.2685
31.6407	1.4655	0.0486	0.0016	0.5190
24.4410	0.9113	0.0539	0.0025	0.3037
17.2351	0.6473	0.0538	0.0019	0.4853
12.2583	0.3507	0.0573	0.0014	0.2277
25.2226	1.0627	0.0500	0.0014	0.4201
25.0815	0.9263	0.0547	0.0026	0.4220
17.0172	0.8109	0.0573	0.0024	0.2179
29.2686	1.4978	0.0491	0.0028	0.5320
29.0851	1.1744	0.0523	0.0025	-0.2174
23.5354	0.8846	0.0507	0.0024	0.2911
50.8241	2.0504	0.0506	0.0024	0.4345
34.0283	1.3121	0.0508	0.0016	0.4420
15.5434	0.7384	0.0555	0.0023	0.3507
22.1734	0.7611	0.0527	0.0022	0.4631
27.7291	1.0855	0.0511	0.0030	0.6290
57.1242	2.1536	0.0485	0.0024	0.4059
25.0676	1.0072	0.0512	0.0015	0.4202
24.5520	0.7590	0.0497	0.0011	0.3616
25.5535	0.9981	0.0507	0.0016	0.4466

31.7529	0.9811	0.0538	0.0013	0.2866
51.0055	2.1861	0.0484	0.0023	0.1708
17.9602	0.6590	0.0533	0.0015	0.5440
31.9780	1.1307	0.0492	0.0022	0.5288
26.8551	1.2257	0.0533	0.0021	0.4028
19.8468	0.6835	0.0538	0.0014	0.4177
38.6443	1.3469	0.0522	0.0027	0.3152
26.1611	0.8586	0.0555	0.0042	0.4847
43.1888	1.3520	0.0504	0.0024	0.0985
11.7106	0.4151	0.0568	0.0013	0.4737
33.6377	1.2764	0.0505	0.0011	0.2292
26.8509	0.7912	0.0529	0.0026	0.1959
23.4026	0.8057	0.0517	0.0020	0.2144
11.3706	0.4752	0.0581	0.0014	0.3997
22.6635	0.8162	0.0517	0.0016	0.1415
50.1967	1.4357	0.0500	0.0017	0.3238
26.0243	0.9364	0.0519	0.0024	0.2240
18.0991	0.6249	0.0545	0.0017	0.2922
26.0748	0.9853	0.0501	0.0019	0.4475
25.9690	1.2443	0.0568	0.0037	0.3708
45.5663	1.6751	0.0462	0.0026	0.0277
20SOZ-03				
25.4872	1.1083	0.0547	0.0026	-0.0769
24.3268	0.8975	0.0519	0.0023	0.3260
25.6396	0.8743	0.0504	0.0015	0.2452
23.6371	1.1099	0.0517	0.0025	-0.0857
23.9294	1.1299	0.0533	0.0020	0.1445
19.4279	0.9140	0.0539	0.0018	0.2033
27.4546	1.4078	0.0523	0.0018	0.3008
18.7196	0.8827	0.0533	0.0016	0.2445
26.9346	0.9605	0.0521	0.0014	0.5508
23.5547	1.0825	0.0520	0.0022	0.4437
23.8931	0.8920	0.0525	0.0028	0.3432
23.2013	1.0986	0.0521	0.0016	-0.1073
17.7592	0.7400	0.0547	0.0018	0.1815
32.8450	1.4129	0.0497	0.0018	0.0082
27.8254	1.2417	0.0517	0.0020	0.5549
26.3954	1.0971	0.0518	0.0016	0.1073
25.4284	1.0600	0.0519	0.0018	0.1692

28.1704	1.4899	0.0499	0.0018	0.5124
17.4353	0.6603	0.0539	0.0021	0.3852
23.9752	1.1792	0.0561	0.0059	-0.5147
24.3283	1.0207	0.0536	0.0021	0.1954
25.0193	1.0556	0.0508	0.0021	0.4114
19.2066	0.8471	0.0542	0.0030	0.4789
25.8281	1.1046	0.0505	0.0015	0.3491
12.8012	0.5356	0.0582	0.0018	0.5135
18.2290	0.8062	0.0541	0.0014	0.0520
26.1692	0.9028	0.0538	0.0022	0.1435
26.5002	1.0109	0.0504	0.0019	0.5411
17.7031	0.6422	0.0541	0.0019	0.1454
13.9785	0.7517	0.0573	0.0019	0.3988
26.6090	1.0768	0.0511	0.0026	-0.0553
26.4971	1.3094	0.0509	0.0021	0.3849
22.7618	1.2082	0.0513	0.0021	0.3246
24.7504	1.2025	0.0523	0.0039	0.2506
12.1973	0.4817	0.0580	0.0026	0.1400
24.9355	1.3471	0.0512	0.0014	0.3495
28.1693	1.3666	0.0515	0.0032	0.2511
24.6729	0.9330	0.0522	0.0017	0.5992
16.4454	0.5757	0.0528	0.0017	0.1258
23.8381	1.0347	0.0541	0.0041	0.2658
17.7705	0.7313	0.0553	0.0021	0.3750
13.5506	0.5431	0.0556	0.0022	0.4266
6.1850	0.3538	0.0739	0.0023	0.5147
24.0127	0.9618	0.0525	0.0026	0.1782
18.5480	0.6617	0.0571	0.0021	0.3054
21.8622	0.9358	0.0535	0.0045	0.3343
20.3439	0.8700	0.0495	0.0061	0.0862
23.4929	0.8973	0.0539	0.0022	0.2558
27.1193	1.4346	0.0514	0.0018	0.5771
23.4621	1.0772	0.0511	0.0033	0.2400
26.3694	1.0499	0.0513	0.0019	0.2282
25.3531	1.4441	0.0543	0.0032	-0.0685
24.3470	1.0909	0.0511	0.0028	0.3726
9.7449	0.4389	0.0604	0.0018	0.3655
17.1060	0.8849	0.0530	0.0021	0.1675
25.1301	1.1939	0.0524	0.0028	0.3318
26.7804	1.5122	0.0511	0.0030	0.3647

27.1498	1.2102	0.0523	0.0019	0.4000
30.7233	1.3572	0.0517	0.0016	0.4387
23.1607	1.1587	0.0519	0.0037	0.3202
25.3223	1.3113	0.0501	0.0013	0.3435
23.2720	1.2134	0.0525	0.0022	0.3633
26.5371	1.0644	0.0529	0.0018	0.4843
25.9008	1.0264	0.0525	0.0014	0.4623
30.8679	0.9006	0.0505	0.0014	0.2501
16.9305	0.8854	0.0530	0.0018	0.6245
6.0151	0.2178	0.0759	0.0013	0.0636
24.6446	0.8332	0.0530	0.0018	0.2813
24.1934	1.0669	0.0519	0.0012	0.2211
25.1903	0.8764	0.0528	0.0019	0.1210
18.0339	0.6276	0.0528	0.0016	0.2466
25.4891	0.7920	0.0512	0.0021	0.3423
16.8886	0.5449	0.0535	0.0014	0.2419
12.5860	0.3966	0.0570	0.0015	0.5980
12.1409	0.5969	0.0562	0.0018	0.5848
12.0889	0.4487	0.0564	0.0025	-0.2270
25.4622	0.8582	0.0520	0.0016	0.4825
12.5796	0.3371	0.0578	0.0018	0.1858
18.9137	0.6472	0.0538	0.0017	0.6574
26.0040	1.0149	0.0517	0.0022	0.7033
13.1346	0.4562	0.0579	0.0019	0.3373
24.1166	0.9148	0.0510	0.0018	-0.2235
24.5397	0.9331	0.0522	0.0034	0.2311
3.3770	0.1247	0.1066	0.0026	0.6393
27.4870	1.0414	0.0522	0.0016	0.3392
27.0669	1.0617	0.0511	0.0013	-0.0751
11.9203	0.4348	0.0565	0.0016	0.1646
25.0947	0.9025	0.0513	0.0015	0.5301
25.0205	0.9028	0.0510	0.0015	0.3668
25.2636	0.8000	0.0525	0.0017	0.4288
22.0096	0.8500	0.0529	0.0015	0.2885
24.5159	0.9801	0.0523	0.0028	0.3603
24.8135	0.9910	0.0490	0.0025	0.0828
23.3667	0.7898	0.0568	0.0030	0.0015
16.9961	0.8318	0.0512	0.0026	-0.0260
22.5559	0.7899	0.0573	0.0041	-0.0412

20SOZ-07				
28.3961	1.3823	0.0489	0.0017	0.0009
24.1391	1.0595	0.0542	0.0020	0.1110
32.1649	1.5848	0.0493	0.0038	0.3156
22.9443	1.3010	0.0542	0.0032	0.5117
25.1067	1.3418	0.0507	0.0022	0.5151
36.1925	1.4047	0.0503	0.0028	0.1079
25.3545	0.9091	0.0519	0.0016	0.3917
28.4165	1.4086	0.0517	0.0021	0.1872
17.3586	0.8319	0.0526	0.0017	0.3072
26.2468	1.4028	0.0506	0.0028	0.5092
23.8617	0.7805	0.0510	0.0027	0.4739
25.1085	1.0952	0.0518	0.0016	0.2390
16.8821	0.6464	0.0535	0.0017	0.4946
33.4396	1.1466	0.0512	0.0034	0.3103
16.2322	0.6185	0.0532	0.0015	0.3848
32.6252	1.2683	0.0487	0.0014	0.0504
18.6925	0.7920	0.0552	0.0016	0.0891
13.3372	0.5235	0.0580	0.0026	0.2645
25.5375	0.9488	0.0508	0.0015	0.3395
27.5052	1.7510	0.0520	0.0030	0.5230
22.6099	0.6986	0.0520	0.0017	0.3186
28.7358	1.3672	0.0525	0.0015	0.3038
26.6413	1.2280	0.0530	0.0021	0.3653
24.7258	0.8094	0.0505	0.0022	0.3394
26.6529	1.6193	0.0526	0.0024	0.3072
36.4276	1.5780	0.0522	0.0027	0.4025
7.5422	0.2845	0.0696	0.0021	0.2593
12.4856	0.5254	0.0571	0.0018	0.2036
5.8022	0.1887	0.0744	0.0024	0.5797
18.1867	0.7354	0.0534	0.0035	0.2581
26.5110	0.8383	0.0516	0.0012	0.3623
31.7859	1.3728	0.0506	0.0023	0.4900
27.7648	1.2699	0.0536	0.0020	0.7045
20SOZ-08B				
22.1102	2.1171	0.0526	0.0049	0.3756
10.2790	0.9326	0.0602	0.0044	-0.1129
23.9549	1.8846	0.0553	0.0051	0.3435
26.0823	2.0019	0.0538	0.0052	0.3442

24.6865	2.8506	0.0478	0.0064	0.4043
17.1755	2.2070	0.0542	0.0050	0.5208
5.2489	0.4891	0.0790	0.0054	0.2242
17.5877	2.1550	0.0513	0.0051	0.4937
17.7498	2.1348	0.0560	0.0054	0.3818
21.4316	1.4609	0.0537	0.0049	0.1517
23.1244	1.6619	0.0515	0.0035	0.4227
25.3675	3.3610	0.0508	0.0065	0.4535
28.0430	3.4517	0.0508	0.0059	0.3233
12.4591	1.4933	0.0584	0.0052	0.6319
25.8142	2.6801	0.0541	0.0051	0.1816
23.1213	2.0836	0.0514	0.0043	0.4565
29.0007	2.3516	0.0502	0.0044	0.6184
32.8220	2.1573	0.0525	0.0031	0.3352
25.5437	2.9873	0.0541	0.0059	0.3699
21.9899	2.7440	0.0496	0.0051	-0.0884
25.7160	2.0810	0.0532	0.0034	0.4574
22.2117	1.4474	0.0513	0.0035	0.4842
23.8814	1.2187	0.0521	0.0029	-0.0201
22.7587	1.3092	0.0501	0.0025	0.3319
24.3626	1.3920	0.0510	0.0017	0.3436
26.0360	0.9918	0.0514	0.0015	0.5414
22.9901	1.0919	0.0521	0.0025	0.4125
29.9182	1.9122	0.0497	0.0020	0.6607
20.8194	1.0867	0.0523	0.0033	0.3682
16.8594	0.8536	0.0536	0.0025	0.2669
22.4168	1.2821	0.0548	0.0051	-0.2809
25.2652	1.3530	0.0506	0.0026	0.6120
24.3095	1.6646	0.0488	0.0035	0.4093
23.1516	1.0682	0.0545	0.0033	0.4561
24.1823	1.2777	0.0507	0.0026	-0.0645
23.4614	1.0806	0.0510	0.0030	0.6551
12.1013	0.4886	0.0589	0.0027	0.4669
29.7534	1.1874	0.0499	0.0023	0.2045
27.2007	1.3237	0.0523	0.0026	0.3615
18.6075	0.6735	0.0538	0.0023	0.5925
12.6615	0.4754	0.0552	0.0021	0.4474
27.9558	1.3422	0.0516	0.0023	0.2447
11.1622	0.5409	0.0574	0.0028	0.2803
25.3995	1.1581	0.0519	0.0015	0.4722

33.9526	1.4977	0.0499	0.0019	0.3821
17.4530	0.8018	0.0542	0.0022	0.5989
26.4915	1.3369	0.0524	0.0019	0.5115
8.0660	0.4103	0.0686	0.0020	0.3411
29.3824	1.5066	0.0499	0.0031	0.4979
25.2295	1.5462	0.0536	0.0024	0.6784
23.9785	1.4001	0.0512	0.0027	0.3431
23.8460	0.9900	0.0484	0.0025	0.4366
29.2124	1.7664	0.0492	0.0026	0.2407
24.4979	0.9362	0.0519	0.0021	0.0137
22.9186	1.0478	0.0545	0.0054	-0.4944
24.8964	1.2333	0.0514	0.0023	0.3748
28.6145	0.9690	0.0519	0.0020	0.4081
5.2836	0.1921	0.0763	0.0040	0.6162
11.5855	0.7294	0.0565	0.0035	0.6581
10.3778	0.5768	0.0600	0.0024	0.1183
11.9635	0.8081	0.0585	0.0031	0.6690
29.7464	1.5439	0.0500	0.0015	0.2855
26.1482	1.3983	0.0512	0.0022	0.1844
28.8566	1.3441	0.0500	0.0026	0.1380
32.2455	1.5122	0.0516	0.0027	0.6633
31.8693	5.0120	0.0554	0.0079	0.3460
22.8451	1.0530	0.0483	0.0016	-0.1536
24.0393	1.6349	0.0567	0.0046	0.1064
24.8360	1.2322	0.0553	0.0043	0.0081
28.5100	3.5745	0.0559	0.0057	0.7883
23.9611	2.5127	0.0565	0.0064	0.4695
15.8614	1.8858	0.0583	0.0063	0.4372
23.4985	3.3575	0.0547	0.0061	0.4553
23.0516	2.7651	0.0557	0.0070	0.4945
27.2087	3.2112	0.0562	0.0067	0.3362
24.5489	2.0230	0.0552	0.0048	0.4614
27.4005	1.2752	0.0558	0.0024	0.5343
11.3990	0.5283	0.0630	0.0025	0.5051
20.3173	0.7952	0.0574	0.0028	0.6527
21.1727	2.5789	0.0558	0.0051	0.3056
23.3103	2.4729	0.0574	0.0064	0.5674
14.0148	1.1613	0.0600	0.0046	0.1579
27.4400	3.5889	0.0543	0.0077	0.5580
19.0960	2.6371	0.0562	0.0080	0.4539

25.3655	3.3476	0.0561	0.0064	0.6331
20SOZ-11B				
25.9846	0.6306	0.0514	0.0021	0.3462
23.9400	0.4853	0.0518	0.0016	0.3671
26.1756	0.8597	0.0545	0.0022	0.2193
23.5595	0.8653	0.0517	0.0018	0.2945
10.2090	0.3644	0.0583	0.0018	0.3658
25.1576	1.0824	0.0531	0.0025	0.2019
29.0732	1.1945	0.0520	0.0042	0.3509
27.9793	1.2680	0.0540	0.0029	-0.0191
27.1655	0.8203	0.0487	0.0024	0.1386
25.9702	1.8046	0.0522	0.0041	0.5020
28.6608	1.3985	0.0547	0.0039	0.3474
16.7842	1.0604	0.0590	0.0037	0.4816
30.7857	1.0005	0.0526	0.0021	0.4093
22.9409	0.7180	0.0499	0.0016	0.3749
29.6959	1.1823	0.0502	0.0033	0.2928
20.9760	0.7843	0.0532	0.0017	0.2882
30.8381	1.0642	0.0542	0.0020	0.1690
22.1567	0.6104	0.0550	0.0033	0.2060
12.4350	0.2180	0.0566	0.0014	0.1046
12.4271	0.3426	0.0608	0.0026	0.3719
25.6590	0.6320	0.0513	0.0016	0.4871
14.8307	0.4106	0.0527	0.0013	0.2223
11.7801	0.4313	0.0558	0.0020	0.5054
23.6224	0.6018	0.0491	0.0014	0.2931
24.7258	0.6216	0.0525	0.0020	0.3017
13.3794	0.4716	0.0569	0.0017	0.0926
28.0001	0.7651	0.0540	0.0013	0.3862
13.3862	0.3795	0.0544	0.0014	0.2295
26.4355	0.8684	0.0527	0.0021	0.4959
18.3726	0.5625	0.0542	0.0021	0.3222
22.5797	0.9350	0.0546	0.0027	0.5070
22.6842	0.8300	0.0526	0.0017	0.3506
26.0138	2.7192	0.0557	0.0049	0.6541
16.3654	1.5032	0.0571	0.0052	0.4430
24.6590	2.5004	0.0502	0.0038	0.3727
16.2685	1.3431	0.0573	0.0049	0.4560
25.7563	2.5235	0.0553	0.0052	0.5548

16.8111	0.9393	0.0545	0.0031	0.3028
5.5047	0.2080	0.0802	0.0043	0.1665
16.2210	0.9369	0.0605	0.0033	0.5553
24.1279	0.8331	0.0513	0.0019	0.1981
22.4262	0.7152	0.0500	0.0017	0.1114
24.6227	1.0238	0.0521	0.0020	0.5224
11.9493	0.3954	0.0572	0.0022	0.5183
29.7487	0.7963	0.0509	0.0031	0.2589
29.2904	0.9456	0.0528	0.0023	0.3747
16.1368	0.5549	0.0548	0.0018	0.6036
24.0253	1.0423	0.0559	0.0041	0.1931
31.1634	1.2135	0.0520	0.0030	0.2385
26.1633	0.8530	0.0509	0.0020	0.3759
17.5681	1.4976	0.0578	0.0024	0.1922
22.7211	0.7115	0.0536	0.0020	0.2461
9.2038	0.2528	0.0617	0.0011	0.2635
27.1660	1.0769	0.0478	0.0012	0.5600
26.0280	1.3471	0.0480	0.0023	0.4599
11.0425	0.3800	0.0552	0.0017	0.2101
58.0670	2.1193	0.0731	0.0124	0.1298
25.5906	1.5062	0.0572	0.0034	0.4813
24.7922	1.4651	0.0836	0.0143	0.1022
14.4885	0.5449	0.0511	0.0016	-0.1890
14.7843	0.4424	0.0513	0.0017	0.1462
27.6012	0.9799	0.0567	0.0029	-0.1310
20.7500	1.0099	0.0589	0.0015	0.1509
13.6506	2.3759	0.2695	0.1070	-0.6692
20SOZ-12				
23.4156	1.0961	0.0550	0.0029	0.2344
26.1070	1.0318	0.0518	0.0033	0.2525
25.9776	1.2420	0.0520	0.0025	0.0919
24.7539	0.9011	0.0538	0.0061	0.4031
5.1448	0.1512	0.0735	0.0028	0.5306
26.8680	1.1536	0.0501	0.0026	0.5700
12.3768	0.4951	0.0555	0.0031	0.3999
23.5951	0.8081	0.0522	0.0026	0.0838
26.7239	0.9436	0.0495	0.0030	0.2403
16.3605	0.5057	0.0542	0.0021	0.4285
25.1667	1.2768	0.0512	0.0020	0.4107

23.8409	0.7058	0.0509	0.0023	0.3760
17.5427	0.5567	0.0539	0.0025	0.2893
27.3600	0.9999	0.0493	0.0021	0.1362
17.6414	0.7022	0.0567	0.0039	0.4572
25.3469	1.1054	0.0565	0.0067	-0.0711
26.8950	1.2028	0.0487	0.0043	0.1314
24.8945	1.0286	0.0509	0.0038	0.4054
25.0878	0.9859	0.0513	0.0018	0.2187
13.1824	0.5023	0.0569	0.0024	0.2254
26.3724	1.0737	0.0500	0.0032	0.3039
10.4703	0.5416	0.0564	0.0027	0.6572
23.8184	1.3769	0.0501	0.0024	0.2173
17.7304	0.7604	0.0536	0.0029	0.6235
8.1847	0.3752	0.0725	0.0031	0.1416
12.4221	0.5556	0.0582	0.0034	0.2861
24.2153	1.0092	0.0525	0.0031	0.3014
16.7238	1.0231	0.0538	0.0026	0.1076
22.3608	0.8539	0.0517	0.0032	0.1443
18.2614	1.1575	0.0510	0.0024	0.3047
23.1258	0.6467	0.0552	0.0029	0.1896
24.5096	1.1596	0.0509	0.0021	0.3392
24.3114	1.2305	0.0511	0.0039	0.3791
12.2129	0.4420	0.0557	0.0028	0.2295
17.1762	0.6837	0.0524	0.0022	0.5610
23.9575	0.7354	0.0512	0.0022	0.5877
23.3581	0.8962	0.0505	0.0038	0.2902
20.6863	0.7958	0.0506	0.0019	0.4152
25.3553	0.8934	0.0510	0.0036	0.4427
16.7808	0.6568	0.0514	0.0023	-0.1165
25.0405	1.2375	0.0533	0.0027	0.3134
26.7198	1.0057	0.0504	0.0032	0.1237
21.9675	0.9801	0.0531	0.0060	-0.1203
17.6519	0.7493	0.0537	0.0021	0.1128
24.5459	1.3133	0.0539	0.0029	0.6879
26.9949	1.2191	0.0522	0.0027	0.0023
25.1006	0.8088	0.0519	0.0024	0.2424
17.0764	0.4937	0.0530	0.0017	0.3026
18.2079	0.5712	0.0525	0.0017	0.5239
32.4406	1.3613	0.0532	0.0028	0.4496
26.2217	1.1119	0.0531	0.0016	0.1121

13.4828	0.5775	0.0633	0.0038	0.3236
27.4950	1.3966	0.0532	0.0030	0.4568
32.4997	1.4816	0.0526	0.0054	0.1283
30.9801	1.2547	0.0532	0.0030	0.4458
21.9998	0.8347	0.0546	0.0037	0.2941
30.9135	1.6771	0.0532	0.0033	0.1920
27.9023	1.2550	0.0510	0.0024	0.1339
27.9242	1.3523	0.0484	0.0030	0.2131
28.2865	1.0800	0.0511	0.0031	0.2867
31.5492	1.4921	0.0504	0.0029	0.5074
20.6239	1.0330	0.0529	0.0028	0.5237
14.5257	0.6278	0.0586	0.0032	0.4008
29.4680	1.3629	0.0532	0.0033	0.4714
14.6492	0.7653	0.0578	0.0028	0.1278
25.6993	1.3170	0.0536	0.0045	0.1590
29.8946	1.6064	0.0528	0.0044	-0.0097
18.1479	1.0895	0.0521	0.0024	0.2531
33.0357	1.6702	0.0524	0.0047	0.1192
28.1455	1.5136	0.0548	0.0046	0.3406
27.2291	1.1172	0.0498	0.0025	0.6328
31.0697	1.0211	0.0497	0.0028	0.2763
28.4706	1.1053	0.0537	0.0035	0.1112
28.6571	0.9607	0.0500	0.0029	0.5132
22.1782	0.9545	0.0538	0.0033	0.2206
30.2307	0.9047	0.0535	0.0031	0.1131
30.1649	0.9629	0.0487	0.0017	0.3210
24.9223	0.8099	0.0508	0.0023	0.4454
14.8334	0.4667	0.0554	0.0032	0.0192
29.4019	0.8422	0.0513	0.0021	0.4275
20.0725	0.7683	0.0561	0.0027	0.5738
28.7531	1.2579	0.0547	0.0035	0.1978
28.9262	1.2919	0.0510	0.0052	0.3019
18.7211	0.8406	0.0546	0.0024	0.3621
10.9121	0.4045	0.0646	0.0031	0.2956
28.2507	1.0870	0.0520	0.0040	0.1850
17.6650	0.6786	0.0505	0.0019	-0.1428
14.8239	0.7271	0.0466	0.0071	0.1448
23.2324	1.2104	0.0481	0.0022	0.4939
8.4898	0.3357	0.0588	0.0024	0.2595
23.9506	0.8894	0.0483	0.0046	0.2457

29.6495	0.8811	0.0457	0.0039	0.2915
24.5088	0.7736	0.0484	0.0038	0.3367
5.1659	0.2216	0.0697	0.0028	0.6075
29.3961	1.3781	0.0573	0.0109	-0.3534
12.5843	0.8686	0.0500	0.0086	0.4089
16.1565	0.8372	0.0679	0.0079	-0.5485
20SOZ-13				
7.0783	0.1825	0.0743	0.0026	0.0490
13.4180	0.4667	0.0636	0.0036	-0.2836
25.7309	0.7883	0.0525	0.0019	0.0554
6.5794	0.2215	0.0695	0.0019	-0.3319
27.4247	0.9966	0.0501	0.0068	0.0649
26.0293	0.7979	0.0546	0.0042	0.4278
25.4181	1.0899	0.0558	0.0023	0.1267
26.9266	0.6652	0.0542	0.0034	0.0960
18.5012	0.5271	0.0533	0.0016	0.4569
28.1421	0.9662	0.0506	0.0029	-0.0363
14.0124	0.3603	0.0583	0.0013	0.3598
28.5634	1.0191	0.0520	0.0049	-0.0369
25.3447	1.0281	0.0508	0.0033	0.2637
27.8428	1.0009	0.0512	0.0023	0.3627
28.3087	1.1255	0.0480	0.0023	-0.1289
12.3509	0.3607	0.0589	0.0022	0.2854
11.8613	0.4418	0.0575	0.0017	0.3106
14.1590	0.3968	0.0580	0.0020	0.1973
28.2207	0.9330	0.0531	0.0037	0.0703
11.9133	0.3784	0.0596	0.0024	0.0621
23.1348	0.8496	0.0527	0.0013	0.5321
27.5906	0.9143	0.0508	0.0026	0.3026
11.9779	0.3473	0.0618	0.0029	0.3457
29.1498	1.0725	0.0532	0.0035	0.1718
28.2147	1.1146	0.0523	0.0021	0.2738
6.5975	0.2544	0.0698	0.0021	0.4849
14.3168	0.4653	0.0558	0.0017	-0.0267
27.9625	0.8116	0.0550	0.0039	0.2907
11.1617	0.3610	0.0584	0.0034	0.3881
24.0913	1.0767	0.0511	0.0017	0.5164
6.9225	0.2139	0.0676	0.0024	0.4047
7.0669	0.2018	0.0786	0.0034	0.1623

6.1898	0.2767	0.0734	0.0029	0.3478
14.1685	0.6415	0.0567	0.0019	0.3167
9.1923	0.3860	0.0621	0.0037	0.0664
27.7868	0.9911	0.0524	0.0034	0.3274
23.0718	0.7341	0.0523	0.0023	-0.0788
25.2372	1.0011	0.0519	0.0048	0.1830
20.6947	0.6490	0.0547	0.0029	-0.0275
7.5165	0.2291	0.0649	0.0033	0.2635
13.3922	0.5866	0.0613	0.0052	0.0004
3.6157	0.1434	0.1059	0.0047	0.2326
28.3806	1.2893	0.0484	0.0032	0.5835
25.0567	0.9175	0.0506	0.0026	0.1689
30.0506	1.0451	0.0508	0.0033	-0.0826
8.0750	0.3747	0.0665	0.0028	0.5748
6.5264	0.1618	0.0786	0.0028	0.1455
31.4213	1.0411	0.0523	0.0051	0.3678
28.5639	1.1506	0.0509	0.0027	-0.2491
23.2626	0.7024	0.0517	0.0027	0.0414
29.6282	0.9115	0.0501	0.0038	-0.0393
19.9975	0.6961	0.0536	0.0030	0.0684
14.9597	0.7027	0.0591	0.0031	0.3147
24.4229	1.1269	0.0563	0.0051	0.2203
25.9755	0.9322	0.0509	0.0025	0.0450
9.5464	1.2827	0.0717	0.0020	0.0026
6.7968	0.2294	0.0772	0.0036	0.3078
25.9153	1.0537	0.0502	0.0053	-0.0350
27.4748	1.1948	0.0548	0.0039	-0.3188
25.9895	0.8217	0.0504	0.0031	0.0727
26.1937	1.0084	0.0552	0.0037	-0.1426
25.0921	0.9390	0.0534	0.0026	0.1282
12.6984	0.4502	0.0606	0.0030	0.3193
27.9905	1.1710	0.0478	0.0057	0.3634
8.3616	0.2664	0.0659	0.0022	0.2440
9.9280	0.5208	0.0581	0.0021	-0.0202
19.7200	0.8109	0.0501	0.0023	0.2105
10.7131	0.3138	0.0589	0.0023	-0.0372
27.5070	0.9811	0.0500	0.0026	0.0001
25.3604	0.7540	0.0529	0.0029	0.1471
18.6122	0.7869	0.0507	0.0015	0.6665
13.9105	0.5015	0.0558	0.0019	0.4925

13.1560	0.5527	0.1671	0.0123	-0.5982
28.5363	1.2331	0.0942	0.0124	-0.7696
12.6018	0.4966	0.0709	0.0049	-0.3018
21.3805	1.3521	0.2324	0.0285	-0.7190
13.0425	0.3414	0.0633	0.0022	0.4528
9.9042	0.4684	0.1156	0.0208	-0.8136
6.5204	0.1666	0.0790	0.0020	0.1999
27.1257	0.8147	0.0587	0.0033	-0.3274
24.9613	1.0834	0.0625	0.0064	-0.0156
19.6022	0.7237	0.0708	0.0054	-0.3451
21.7838	0.7656	0.1541	0.0158	-0.5169
16.8576	0.7902	0.0736	0.0044	0.0022
27.0084	0.9649	0.0673	0.0067	0.1402
10.5922	0.9562	0.2227	0.0426	-0.8507
20.5562	0.8940	0.2059	0.0160	-0.4139
12.4619	0.5569	0.0673	0.0078	-0.0488
22.2024	1.2007	0.1125	0.0087	-0.2383
22.6779	0.7272	0.0595	0.0052	0.0118
27.3079	0.8294	0.0768	0.0055	-0.5088
28.2535	1.2182	0.0609	0.0067	-0.0166
15.7462	0.5493	0.0616	0.0042	-0.0775
31.8984	2.1634	0.0591	0.0052	-0.0530
25.5690	1.3484	0.0809	0.0165	-0.6008
29.8226	1.1040	0.0465	0.0054	0.3188
3.0978	0.0840	0.1402	0.0080	0.4931
5.0698	0.1844	0.1199	0.0067	-0.3926
13.2306	0.5321	0.0696	0.0062	-0.3273
22.9072	0.6746	0.0856	0.0067	-0.2088
20SOZ-14				
16.1060	0.6344	0.0534	0.0022	0.1018
19.3758	1.1501	0.0514	0.0013	0.4296
5.9490	0.1471	0.0729	0.0025	0.0917
4.6034	0.1666	0.0786	0.0026	0.3661
25.2804	0.7350	0.0495	0.0023	0.0035
5.6904	0.1282	0.0777	0.0030	-0.0226
6.0931	0.2384	0.0709	0.0034	0.0662
23.8725	0.9958	0.0515	0.0024	0.1982
25.7473	0.9284	0.0546	0.0034	0.3138
11.3205	0.3277	0.0575	0.0021	0.1614

9.9472	0.3710	0.0613	0.0023	0.3510
18.3856	0.7412	0.0515	0.0035	0.3978
15.7779	0.6798	0.0541	0.0023	-0.0230
20.3416	0.6909	0.0514	0.0027	0.4760
22.6792	0.6926	0.0502	0.0016	0.2710
5.3494	0.2132	0.0872	0.0054	0.4555
10.1126	0.3510	0.0616	0.0026	0.3291
15.4192	0.5203	0.0543	0.0019	0.3937
11.3891	0.3694	0.0607	0.0022	0.3460
13.0192	0.4039	0.0614	0.0026	0.3552
52.3947	1.6548	0.0480	0.0024	0.4149
8.3149	0.3989	0.0679	0.0025	-0.0817
16.6277	0.4743	0.0544	0.0025	0.0503
18.8270	0.5699	0.0514	0.0016	0.3292
12.8156	0.4644	0.0573	0.0023	0.3974
9.3337	0.2793	0.0611	0.0025	0.0376
19.2328	0.5610	0.0540	0.0026	0.1938
17.1543	0.5962	0.0559	0.0021	0.2375
24.2222	0.7110	0.0507	0.0020	0.1711
13.8266	0.3810	0.0559	0.0020	0.3136
12.0415	0.3992	0.0594	0.0023	0.4904
18.6511	0.5844	0.0548	0.0022	-0.1110
24.6943	0.9321	0.0537	0.0022	0.0936
60.1413	2.5400	0.0508	0.0053	0.3387
6.6889	0.3410	0.0697	0.0025	0.1586
19.3501	0.7785	0.0537	0.0021	0.2675
57.7900	3.2935	0.0492	0.0034	0.0450
24.3491	1.1967	0.0517	0.0076	0.0321
24.7304	0.9227	0.0543	0.0032	0.2583
58.7400	2.2607	0.0486	0.0040	0.0213
11.9374	0.4640	0.0587	0.0032	0.3779
15.8452	0.4462	0.0552	0.0024	0.3575
13.0442	0.3757	0.0591	0.0041	0.3184
47.5587	1.3425	0.0496	0.0023	0.3866
11.8353	0.4727	0.0574	0.0016	0.4678
24.7810	0.7705	0.0524	0.0028	0.4350
19.6533	1.5451	0.0537	0.0029	-0.4013
11.6729	2.9533	0.0665	0.0035	-0.7642
51.3931	2.0175	0.0476	0.0033	0.1986
15.5727	0.5084	0.0550	0.0020	0.4662

15.9293	0.7389	0.0583	0.0026	-0.2604
11.0488	0.2976	0.0603	0.0037	0.1931
5.7038	0.2350	0.0710	0.0056	0.0464
15.9206	0.5083	0.0550	0.0021	0.1334
11.0560	0.3647	0.0570	0.0023	0.5323
55.2364	1.4192	0.0505	0.0047	-0.0623
18.7795	0.7877	0.0527	0.0020	0.4077
17.4071	0.8531	0.0527	0.0023	0.2857
55.5821	1.8602	0.0528	0.0039	0.4399
3.4673	0.1043	0.1042	0.0025	0.4991
17.2038	0.4869	0.0528	0.0034	0.4167
23.9175	0.8928	0.0516	0.0044	0.2215
12.6676	0.6012	0.0613	0.0024	-0.0735
16.9042	0.6761	0.0565	0.0035	0.5061
17.2688	0.6943	0.0528	0.0022	0.0543
11.5576	0.5181	0.0586	0.0032	0.5346
20.2250	1.0080	0.0530	0.0033	0.0165
12.5291	0.5785	0.0591	0.0024	0.3246
11.7247	0.5274	0.0610	0.0031	0.1172
27.7156	1.6018	0.0518	0.0040	0.4298
53.7559	2.8351	0.0504	0.0047	0.1437
15.2076	0.8377	0.0536	0.0023	0.3453
24.3988	1.9961	0.0490	0.0033	0.0163
52.4068	2.7230	0.0478	0.0036	0.4162
24.7305	1.4182	0.0503	0.0029	0.1633
11.6984	0.5805	0.0626	0.0042	0.0326
12.2425	0.6533	0.0577	0.0040	0.4253
23.2773	1.2140	0.0537	0.0034	0.4907
50.9385	2.2749	0.0480	0.0030	0.2724
29.8247	1.0808	0.0505	0.0022	0.2138
11.2589	0.3500	0.0584	0.0064	0.3202
13.3570	0.6250	0.0549	0.0022	0.2856
19.0011	0.6080	0.0530	0.0023	0.0249
57.5543	2.4349	0.0519	0.0072	0.1200
58.1250	2.1761	0.0468	0.0055	0.4476
13.3572	0.4394	0.0566	0.0023	0.5577
15.0071	0.4704	0.0535	0.0024	0.2776
56.2487	1.9732	0.0480	0.0058	0.0448
14.7326	0.3626	0.0521	0.0014	0.1800
15.5301	0.5873	0.0549	0.0023	0.5691

28.2925	1.0417	0.0516	0.0029	0.3423
52.3827	1.5343	0.0721	0.0224	-0.4066
10.2990	0.3806	0.0561	0.0020	0.2642
6.3031	0.7052	0.0908	0.0051	-0.6919
58.4724	3.4196	0.0455	0.0046	0.1632
15.1413	0.9587	0.0516	0.0025	0.3957
23.1603	1.2107	0.0499	0.0041	0.4286
55.2444	2.5848	0.0718	0.0072	0.2731
5.4338	0.2306	0.6299	0.0247	0.4093
59.6912	1.5223	0.0609	0.0052	0.2693
20SOZ-15				
2.9121	0.1110	0.1198	0.0032	0.3377
10.8194	0.4796	0.0625	0.0014	0.2789
10.0336	0.3601	0.0571	0.0019	0.2372
22.6230	0.8441	0.0507	0.0017	0.6511
5.2009	0.1818	0.0723	0.0019	0.6716
5.1860	0.1494	0.0717	0.0021	0.3913
5.4077	0.1799	0.0803	0.0023	0.4825
4.5961	0.1860	0.0957	0.0043	0.1621
22.5866	1.0781	0.0524	0.0019	0.5945
25.6378	1.4657	0.0531	0.0054	0.2306
2.8005	0.1902	0.1287	0.0049	-0.0656
12.4356	1.5436	0.0618	0.0032	-0.6002
6.9148	0.1919	0.0669	0.0017	-0.0396
15.8272	0.6055	0.0545	0.0018	-0.1153
3.5628	0.1695	0.1058	0.0035	0.1550
56.2938	2.1221	0.0495	0.0035	0.2391
3.2234	0.1649	0.1122	0.0036	-0.0830
15.4667	0.6210	0.0530	0.0019	0.1673
67.5596	2.9479	0.0487	0.0035	0.1851
66.0302	2.2907	0.0494	0.0030	0.0588
16.0532	0.8526	0.0545	0.0025	0.5861
15.6057	0.9829	0.0578	0.0049	0.5308
15.5870	0.8696	0.0542	0.0023	0.2479
48.5968	3.1237	0.0508	0.0041	0.4118
14.5714	0.9112	0.0547	0.0042	0.4339
46.2107	2.4179	0.0505	0.0033	0.1452
15.9131	1.0921	0.0548	0.0041	0.1864
13.8899	1.5559	0.0565	0.0056	0.4150

10.1931	1.1097	0.0640	0.0068	0.4767
10.6135	1.1860	0.0614	0.0065	0.5930
9.8586	1.0465	0.0651	0.0067	0.5165
19.4753	1.4589	0.0522	0.0039	0.2352
9.2999	0.4800	0.0589	0.0036	0.3017
16.1383	1.1889	0.0546	0.0041	0.2138
49.5879	3.5815	0.0525	0.0045	0.2411
8.3835	0.4076	0.0645	0.0040	0.2864
40.6617	1.8153	0.0511	0.0030	0.3741
16.6550	1.0758	0.0583	0.0032	0.5901
15.4426	0.7170	0.0544	0.0015	0.4710
16.3642	0.6298	0.0530	0.0015	0.3167
5.5133	0.3569	0.0744	0.0047	0.2199
4.6040	0.1963	0.0830	0.0028	0.3000
4.5534	0.2343	0.0776	0.0025	0.3661
14.1902	0.8617	0.0600	0.0043	-0.2953
15.3471	0.5399	0.0605	0.0024	0.0278
19.7697	1.1895	0.0558	0.0025	0.4549
2.3980	0.1488	0.1761	0.0069	0.0966
51.8453	2.1332	0.0493	0.0025	0.2586
10.1741	0.3255	0.0571	0.0025	0.4883
17.7944	1.0125	0.0533	0.0032	0.4092
15.0251	0.5602	0.0552	0.0021	0.5000
2.9658	0.1609	0.1108	0.0040	0.4785
6.3785	0.4753	0.0703	0.0028	-0.3610
10.3217	0.3962	0.0554	0.0027	0.2237
15.2394	0.4576	0.0547	0.0021	0.3978
8.3387	0.2633	0.0662	0.0018	0.0880
16.3598	0.5182	0.0557	0.0025	0.0018
10.0430	0.3520	0.0603	0.0022	0.0386
9.4867	0.5479	0.0666	0.0029	-0.1762
44.6281	1.3806	0.0473	0.0014	0.1936
9.5480	0.3730	0.0594	0.0016	0.0827
9.7328	0.3006	0.0578	0.0016	0.3894
13.6184	1.1259	0.0544	0.0017	0.3639
11.5208	0.4562	0.0567	0.0020	0.7245
14.3859	0.6053	0.0550	0.0014	0.2133
2.8301	0.1098	0.1361	0.0048	-0.0268
16.9336	0.6666	0.0522	0.0015	0.6524
10.2832	0.6027	0.0627	0.0015	-0.0215

5.1184	0.2540	0.0738	0.0027	0.6555
10.2347	0.4110	0.0564	0.0017	0.4834
53.9008	2.3185	0.0522	0.0022	0.3352
45.5956	1.6796	0.0465	0.0016	0.2384
5.4829	0.2237	0.0738	0.0028	0.6316
14.8908	0.4678	0.0535	0.0015	0.4097
14.4067	0.6171	0.0524	0.0015	0.3729
17.4484	0.7101	0.0518	0.0022	0.3955
15.4236	0.8584	0.0522	0.0022	0.6763
53.5714	2.5072	0.0498	0.0035	0.4096
49.7128	3.8550	0.0511	0.0039	0.5793
17.4033	1.2237	0.0550	0.0053	0.4485
4.6861	0.3559	0.0769	0.0067	0.5569
12.5947	1.2318	0.0589	0.0064	0.5711
55.1121	4.9478	0.0502	0.0057	0.4474
5.2948	0.4535	0.0772	0.0073	0.5152
19.5252	1.3640	0.0511	0.0030	0.1953
3.0787	0.2139	0.1891	0.0059	0.0545
5.4555	0.3019	0.0684	0.0015	0.1144
24.0599	1.2159	0.0582	0.0029	0.6322
5.6302	0.4436	0.1069	0.0108	0.0938
2.2937	0.1335	0.2727	0.0093	0.1282
3.3887	0.1845	0.1663	0.0058	0.3814
14.6751	0.3973	0.0511	0.0015	0.2150
14.3503	0.5202	0.0519	0.0016	0.3415
14.1005	0.6535	0.0523	0.0021	0.1640
9.3473	0.2996	0.0564	0.0023	0.4367
12.5246	1.0490	0.0649	0.0065	0.4884
5.0175	0.3336	0.0691	0.0036	0.6362
20SOZ-16				
17.4030	0.5746	0.0534	0.0021	0.2332
19.6081	0.5120	0.0544	0.0022	0.1033
11.3927	0.3723	0.0565	0.0023	0.0094
10.7885	0.3842	0.0591	0.0018	0.3210
57.1113	2.0105	0.0486	0.0025	0.1087
9.8979	0.3088	0.0588	0.0021	0.6481
18.2499	0.6661	0.0535	0.0025	0.1571
18.5841	0.5921	0.0557	0.0030	0.4505
5.5043	0.1584	0.0708	0.0020	0.3396

8.0602	0.3092	0.0726	0.0030	0.1595
18.1066	0.6755	0.0555	0.0020	0.2551
5.4939	0.2035	0.0778	0.0024	0.2886
5.6459	0.1915	0.0760	0.0021	0.2869
11.3532	0.3706	0.0570	0.0013	0.2743
11.2868	0.3267	0.0602	0.0023	0.1836
17.8182	0.7419	0.0559	0.0024	0.3876
52.7553	1.8227	0.0490	0.0027	0.5596
50.8156	1.5420	0.0497	0.0026	0.2760
5.7004	0.1976	0.0859	0.0024	0.2787
10.9365	0.3012	0.0592	0.0055	0.2207
6.6053	0.2068	0.0749	0.0027	0.5083
8.6934	0.3631	0.0618	0.0024	0.2349
5.3882	0.1851	0.0723	0.0018	0.3067
5.8405	0.2632	0.0744	0.0026	0.5687
7.4608	0.3670	0.0657	0.0022	0.5331
17.1540	0.6199	0.0554	0.0031	0.0412
6.8634	0.3640	0.0749	0.0016	0.4424
12.2227	0.4526	0.0635	0.0060	-0.0633
10.1036	0.3414	0.0605	0.0020	0.3950
17.8844	0.7151	0.0549	0.0026	0.3911
5.3464	0.1577	0.0718	0.0023	0.5785
38.2022	1.2294	0.0479	0.0042	0.2696
2.5197	0.1033	0.1497	0.0056	0.5205
6.1492	0.2019	0.0677	0.0019	0.3793
16.7162	0.6033	0.0539	0.0021	0.6565
11.0795	0.5154	0.0600	0.0048	0.1705
18.6440	0.5283	0.0542	0.0014	0.3388
55.3843	2.0688	0.0467	0.0066	0.1527
13.7435	0.5860	0.0579	0.0021	0.3210
60.6925	2.3756	0.0496	0.0048	0.0852
2.3742	0.0753	0.1454	0.0040	0.5690
5.8669	0.1577	0.0730	0.0018	0.3732
5.6486	0.2398	0.0721	0.0027	0.5792
18.7943	0.5734	0.0532	0.0022	0.1116
17.5307	0.6369	0.0527	0.0017	0.4487
10.4388	0.4247	0.0636	0.0018	0.3588
4.9907	0.1410	0.0769	0.0039	0.0641
10.4270	0.3880	0.0571	0.0020	0.5353
18.8249	0.7191	0.0508	0.0026	0.2722

55.4361	2.1724	0.0471	0.0017	0.5479
9.7764	0.8464	0.0546	0.0123	0.2793
56.5670	2.0222	0.0541	0.0089	0.1496
57.5204	2.5872	0.0578	0.0085	0.0942
49.6942	1.9267	0.0568	0.0064	-0.1328
6.3688	0.3963	0.1415	0.0298	-0.7239
59.2221	2.4414	0.0540	0.0081	-0.1051
8.5716	0.3373	0.0736	0.0034	0.1320
20SOZ-19				
33.0168	1.4202	0.0481	0.0017	-0.0026
21.8695	0.9138	0.0574	0.0029	0.3410
17.7115	0.7971	0.0537	0.0021	0.0566
30.8654	1.2528	0.0487	0.0025	0.2438
5.8680	0.3929	0.0789	0.0032	0.3018
17.6189	0.6707	0.0529	0.0019	0.2648
12.1452	0.5079	0.0555	0.0021	0.3750
18.9489	0.7502	0.0528	0.0022	0.3664
24.8531	0.9975	0.0515	0.0028	0.1870
5.5175	0.2171	0.0706	0.0030	0.1578
11.1650	0.4122	0.0575	0.0021	0.3968
8.4398	0.4386	0.0694	0.0037	0.7366
10.8793	0.4826	0.0604	0.0027	0.4778
23.5157	0.9166	0.0527	0.0022	0.3768
13.8041	0.8576	0.0624	0.0031	0.3156
29.0346	1.1788	0.0532	0.0031	0.5133
21.9345	1.3319	0.0496	0.0029	0.4461
10.2982	0.5923	0.0570	0.0022	0.4720
22.6834	1.2766	0.0549	0.0026	0.5531
21.2327	0.9004	0.0540	0.0026	0.4072
13.0934	0.5778	0.0556	0.0022	0.3023
13.9442	0.6448	0.0543	0.0024	0.2169
25.0477	1.1800	0.0517	0.0026	0.0824
22.7037	1.0316	0.0507	0.0028	0.4398
32.7487	1.4847	0.0483	0.0021	-0.0490
16.7259	0.9264	0.0526	0.0027	0.4240
10.5501	0.4610	0.0568	0.0026	0.5595
23.1835	0.9563	0.0536	0.0036	0.5532
20.6589	0.9486	0.0502	0.0015	0.1502
20.9753	1.1495	0.0501	0.0018	0.2633

9.1994	0.3872	0.0605	0.0027	0.5505
24.4883	1.0853	0.0510	0.0019	0.3526
19.4502	0.8431	0.0497	0.0025	0.7343
27.2208	1.1321	0.0547	0.0024	0.2503
23.9966	0.9844	0.0516	0.0024	0.3183
5.5787	0.2668	0.0759	0.0023	0.3534
22.6225	0.8390	0.0520	0.0031	0.2305
10.6858	0.3842	0.0575	0.0017	0.7129
2.8825	0.0838	0.1140	0.0037	0.3743
30.1745	1.0929	0.0502	0.0032	0.1807
8.2307	0.3902	0.0645	0.0029	0.2281
6.6897	0.3193	0.0761	0.0030	0.0002
22.2111	1.2731	0.0510	0.0025	0.1930
33.8609	1.3232	0.0487	0.0016	0.2750
23.3674	0.8448	0.0502	0.0018	0.3464
1.5796	0.0627	0.2225	0.0066	0.2858
25.9223	1.0817	0.0536	0.0037	0.0253
11.1793	0.4564	0.0556	0.0019	0.3241
24.8907	0.8034	0.0537	0.0033	0.2702
11.1501	0.3453	0.0577	0.0028	0.4515
21.0670	0.7389	0.0512	0.0020	0.6410
26.1932	1.0626	0.0500	0.0021	0.5160
7.2462	0.3437	0.0682	0.0026	-0.1557
5.2294	0.1758	0.0752	0.0020	0.1655
16.5563	0.6760	0.0510	0.0016	-0.0124
12.7352	0.6000	0.0589	0.0032	0.5805
21.4142	1.0774	0.0507	0.0025	0.6510
9.7121	0.5177	0.0604	0.0016	0.4164
9.2798	0.3439	0.0592	0.0016	0.4074
21.6795	0.9799	0.0495	0.0021	0.3447
29.2610	1.0855	0.0517	0.0022	0.3420
22.0635	0.7674	0.0516	0.0018	0.0068
13.9969	1.3557	0.0611	0.0024	-0.0985
6.6961	0.3565	0.0770	0.0026	0.3638
7.7314	0.9090	0.0696	0.0034	-0.3691
12.0735	0.3492	0.0550	0.0022	0.4931
27.3457	0.9752	0.0489	0.0017	0.2797
10.3373	0.4110	0.0575	0.0016	0.4035
46.4502	1.7625	0.0469	0.0024	0.3835
23.3121	1.0890	0.0505	0.0020	-0.1504

41.2773	1.3330	0.0502	0.0025	-0.0441
38.6571	1.6805	0.0481	0.0032	-0.0601
33.5074	1.0614	0.0533	0.0038	0.5053
47.2646	1.5316	0.0473	0.0022	0.0961
52.3920	2.0067	0.0470	0.0024	0.3064
17.4063	0.6103	0.0559	0.0018	0.2576
25.5802	0.7947	0.0528	0.0018	0.1932
26.4355	0.8946	0.0538	0.0032	0.3105
17.9170	0.7337	0.0547	0.0022	0.3815
54.8714	2.4518	0.0523	0.0025	0.1251
46.3080	1.7156	0.0496	0.0026	-0.0345
55.8033	2.1499	0.0515	0.0020	0.1858
12.0791	0.4790	0.0591	0.0017	0.2926
42.7547	1.5638	0.0514	0.0024	-0.0102
24.9807	1.1545	0.0687	0.0058	0.2437
25.5207	1.0112	0.0691	0.0040	0.2578
19.8120	0.6158	0.0496	0.0024	0.4075
18.5041	1.5682	0.0873	0.0115	-0.7113
2.9425	0.6738	0.3965	0.0925	-0.9590
25.6711	1.2374	0.0473	0.0020	0.5352
19.6564	0.6356	0.0639	0.0063	0.0192
19.2463	0.8778	0.1095	0.0120	-0.2835
8.4493	0.3955	0.0581	0.0022	0.2257
16.8294	2.8087	0.0885	0.0117	-0.8649
47.5102	2.3919	0.0569	0.0037	-0.2016
11.4587	0.4629	0.0544	0.0021	0.2877
25.0631	1.1374	0.0481	0.0018	0.4396
9.8806	0.3708	0.0560	0.0019	0.3718
20.6113	0.7174	0.0898	0.0046	0.0798
23.3922	0.7991	0.0593	0.0029	-0.3276
24.9807	1.1545	0.0687	0.0058	0.2437
20SOZ-21				
32.6503	1.3148	0.0508	0.0018	0.4748
34.7982	1.6667	0.0521	0.0045	0.5525
16.3188	0.5030	0.0563	0.0017	0.2732
13.5553	0.4050	0.0535	0.0015	0.2037
45.1544	2.2857	0.0518	0.0029	0.2943
41.4732	1.6531	0.0502	0.0025	0.5506
18.4112	0.5719	0.0542	0.0015	0.1402

16.9900	0.8790	0.0525	0.0019	0.3332
52.6219	2.1321	0.0467	0.0030	0.0417
10.1067	0.5630	0.0601	0.0022	0.6354
26.6790	1.0420	0.0518	0.0023	0.2776
23.8945	0.8749	0.0501	0.0020	0.3560
27.1611	1.0038	0.0522	0.0043	0.2751
26.2958	0.9932	0.0497	0.0031	0.1202
23.3180	0.9789	0.0499	0.0026	0.2223
18.0543	0.5631	0.0530	0.0017	-0.4523
37.7961	1.6592	0.0469	0.0036	0.2324
16.3747	0.5226	0.0529	0.0018	0.6653
24.2102	1.0156	0.0504	0.0018	0.1279
43.9892	1.4561	0.0475	0.0014	0.3455
7.6949	0.3596	0.0720	0.0024	-0.0554
24.8684	1.1583	0.0533	0.0020	0.6082
16.7448	0.5409	0.0527	0.0025	-0.1353
20.6006	0.6981	0.0564	0.0036	0.0780
23.3108	0.8015	0.0500	0.0018	0.0028
17.3132	0.6748	0.0556	0.0017	-0.0378
9.1380	0.2271	0.0564	0.0030	0.2301
20.3997	0.7760	0.0505	0.0012	0.5369
52.7729	1.6028	0.0491	0.0026	-0.0910
26.4553	0.9762	0.0513	0.0020	0.3925
46.4840	2.1121	0.0474	0.0018	0.1560
51.0570	1.4575	0.0495	0.0029	0.1513
53.4643	2.5140	0.0483	0.0036	0.3183
22.7112	0.7375	0.0523	0.0021	-0.0653
45.2565	1.5105	0.0466	0.0020	0.3022
25.0191	0.8875	0.0519	0.0021	0.4551
37.4978	1.0205	0.0481	0.0019	0.3250
16.5989	0.6625	0.0528	0.0019	0.2689
24.9044	0.8893	0.0510	0.0020	0.4052
48.7646	1.6839	0.0467	0.0028	0.4517
55.4946	1.8803	0.0461	0.0030	0.4180
22.1841	0.8326	0.0503	0.0015	0.1569
17.6213	0.6493	0.0530	0.0016	0.2695
31.4721	0.8815	0.0496	0.0020	0.0317
28.1218	0.9661	0.0522	0.0028	0.2657
26.0220	0.9526	0.0516	0.0040	0.1040
52.6320	2.1501	0.0491	0.0037	0.4801

5.9910	0.2279	0.0750	0.0024	0.5280
16.3741	0.7681	0.0515	0.0024	0.2852
6.0950	0.2308	0.0765	0.0027	0.3127
25.1697	0.8555	0.0530	0.0040	0.1284
56.9657	2.7605	0.0486	0.0021	0.3948
51.2514	2.1537	0.0529	0.0054	0.2021
12.7372	0.4545	0.0567	0.0020	-0.2320
44.1759	1.5897	0.0481	0.0020	0.4831
24.3697	0.6335	0.0518	0.0026	0.3596
23.5476	0.8076	0.0529	0.0024	0.3928
55.7662	2.0233	0.0474	0.0041	0.0712
13.0671	0.3715	0.0563	0.0019	0.4424
25.8631	0.9597	0.0530	0.0034	0.1967
23.9230	0.7285	0.0519	0.0022	0.5747
50.8640	2.1454	0.0485	0.0025	0.4528
29.6754	0.9567	0.0500	0.0030	0.4071
26.9838	0.9221	0.0513	0.0026	0.4353
45.3528	1.2776	0.0485	0.0016	0.5985
51.8191	1.9741	0.0521	0.0033	0.3126
51.4439	1.7360	0.0478	0.0029	-0.1000
5.2507	0.1974	0.0751	0.0024	0.6445
43.8741	1.5749	0.0497	0.0028	0.1987
34.7809	1.2447	0.0548	0.0042	0.3539
49.1153	1.4549	0.0493	0.0013	0.1336
23.8342	0.7487	0.0528	0.0020	0.1811
23.1932	1.0310	0.0521	0.0018	0.5126
12.0735	0.3492	0.0550	0.0022	0.4931
27.3457	0.9752	0.0489	0.0017	0.2797
10.3373	0.4110	0.0575	0.0016	0.4035
46.4502	1.7625	0.0469	0.0024	0.3835
23.3121	1.0890	0.0505	0.0020	-0.1504
41.2773	1.3330	0.0502	0.0025	-0.0441
38.6571	1.6805	0.0481	0.0032	-0.0601
33.5074	1.0614	0.0533	0.0038	0.5053
47.2646	1.5316	0.0473	0.0022	0.0961
52.3920	2.0067	0.0470	0.0024	0.3064
17.4063	0.6103	0.0559	0.0018	0.2576
25.5802	0.7947	0.0528	0.0018	0.1932
26.4355	0.8946	0.0538	0.0032	0.3105
17.9170	0.7337	0.0547	0.0022	0.3815

54.8714	2.4518	0.0523	0.0025	0.1251
46.3080	1.7156	0.0496	0.0026	-0.0345
55.8033	2.1499	0.0515	0.0020	0.1858
12.0791	0.4790	0.0591	0.0017	0.2926
42.7547	1.5638	0.0514	0.0024	-0.0102
45.3930	3.6614	0.1638	0.0424	-0.7497
21.5611	0.8644	0.1263	0.0074	0.4246
24.9555	0.6633	0.0716	0.0070	0.0245
59.4114	2.1478	0.0453	0.0038	0.0322
39.7347	2.1997	0.0769	0.0076	-0.2513
46.6825	1.6928	0.0577	0.0032	0.3830
17.0237	0.3825	0.0706	0.0025	0.6085
24.9807	1.1545	0.0687	0.0058	0.2437

References

Adams, C.J., Campbell, H.J., Graham, I.J. and Mortimer, N., 1998. Torlesse, Waipapa and Caples suspect terranes of New Zealand: integrated studies of their geological history in relation to neighbouring terranes. *EpisodesJournal of International Geoscience*, *21*(4), pp.235-240.

Adams, C.J., Barley, M.E., Maas, R. and Doyle, M.G., 2002. Provenance of Permian-Triassic volcaniclastic sedimentary terranes in New Zealand: evidence from their radiogenic isotope characteristics and detrital mineral age patterns. *New Zealand Journal of Geology and Geophysics*, *45*(2), pp.221-242.

Adams, C.J., Campbell, H.J. and Griffin, W.L., 2007. Provenance comparisons of Permian to Jurassic tectonostratigraphic terranes in New Zealand: perspectives from detrital zircon age patterns. *Geological Magazine*, *144*(4), pp.701-729.

Adams, C.J., Mortimer, N., Campbell, H.J. and Griffin, W.L., 2015. Detrital zircon ages in Buller and Takaka terranes, New Zealand: constraints on early Zealandia history. *New Zealand Journal of Geology and Geophysics*, *58*(2), pp.176-201.

Adams, C.J., Campbell, H.J., Mortimer, N. and Griffin, W.L., 2017. Perspectives on Cretaceous Gondwana break-up from detrital zircon provenance of southern Zealandia sandstones. *Geological Magazine*, *154*(4), pp.661-682.

Allibone, A.H., MacKenzie, D., Turnbull, R., Tulloch, A. and Craw, D., 2016. Polymetallic mineralisation associated with Carboniferous I-type granitoids in central Stewart Island, New Zealand. *New Zealand Journal of Geology and Geophysics*, *59*(3), pp.436-456.

Allibone, A.H. and Tulloch, A.J., 2004. Geology of the plutonic basement rocks of Stewart Island, New Zealand. *New Zealand Journal of Geology and Geophysics*, *47*(2), pp.233-256.

Buriticá, L.F., Schwartz, J.J., Klepeis, K.A., Miranda, E.A., Tulloch, A.J., Coble, M.A. and Kylander-Clark, A.R., 2019. Temporal and spatial variations in magmatism and transpression in a Cretaceous arc, Median Batholith, Fiordland, New Zealand. *Lithosphere*, *11*(5), pp.652-682.

Bolhar, R., Weaver, S.D., Palin, J.M., Cole, J.W. and Paterson, L.A., 2008. Systematics of zircon crystallisation in the Cretaceous Separation Point Suite, New Zealand, using U/Pb isotopes, REE and Ti geothermometry. *Contributions to Mineralogy and Petrology*, *156*(2), pp.133-160.

Bourdon, B., Turner, S., Henderson, G.M. and Lundstrom, C.C., 2003. Introduction to U-series geochemistry. *Reviews in mineralogy and geochemistry*, *52*(1), pp.1-21.

Cawood, P.A., Nemchin, A.A., Freeman, M. and Sircombe, K., 2003. Linking source and sedimentary basin: Detrital zircon record of sediment flux along a modern river system and implications for provenance studies. *Earth and Planetary Science Letters*, *210*(1-2),pp.259-268.

A: Campbell, M.J., Rosenbaum, G., Allen, C.M. and Mortimer, N., 2020. *Origin of dispersed Permian–Triassic fore-arc basin terranes in New Zealand: Insights from zircon petrochronology. Gondwana Research,* 78, pp.210-227

B: campbell, M.J., Rosenbaum, G., Allen, C.M., Mortimer, N. and Shaanan, U., 2020. *Episodic behavior of theeastern Gondwanan margin: Insights from detrital zircon petrochronology from the Murihiku Terrane, New Zealand. Lithos,* 356, p.105367

C: Campbell , M.J., Rosenbaum, G., Allen, C.M. and Spandler, C., 2020. *Continental crustal growth processes revealed by detrital zircon petrochronology: Insights from Zealandia. Journal of Geophysical Research:* Solid Earth, 125(8), p.e2019JB019075.

Chew, D.M., Petrus, J.A. and Kamber, B.S., 2014. U–Pb LA–ICPMS dating using accessory mineral standards with variable common Pb. *Chemical Geology*, *363*, pp.185-199.

Chew, D., O'Sullivan, G., Caracciolo, L., Mark, C. and Tyrrell, S., 2020. Sourcing the sand: Accessory mineral fertility, analytical and other biases in detrital U-Pb provenance analysis. *Earth-Science Reviews*, *202*, p.103093.

Compston, W. and Pidgeon, R.T., 1986. *Jack Hills, evidence of more very old detrital zircons in Western Australia. Nature,* 321(6072), pp.766-769.

Coney, P.J., Jones, D.L. and Monger, J.W., 1980. Cordilleran suspect terranes. *Nature*, *288*(5789), pp.329-333.

Davids, C., 1999. A Thermochronological Study of Southern Fiordland, New Zealand [Ph. D. thesis].

Decker, M.F.I., 2016. *Triggering mechanisms for a magmatic flare-up of the lower crust in Fiordland, New Zealand, from U-Pb zircon geochronology and O-Hf zircon geochemistry* (Doctoral dissertation, California State University, Northridge).

Dickinson, W.R., and Gehrels, G.E., 2009, U-Pb ages of detrital zircons in Jurassic eolian and associated sandstones of the Colorado Plateau—Evidence for transcontinental dispersal and intraregional recycling of sediment: Geological Society of America Bulletin, v. 121, p. 408–433, doi:10.1130/B26406.1.

Edbrooke, S.W., 2017. *The Geological Map of New Zealand: To accompany Geological Map of New Zealand 1: 1 000 000*. GNS Science.

Gehrels, G.E., 2000. Introduction to detrital zircon studies of Paleozoic and Triassic strata in western Nevada and northern California. *Special Paper of the Geological Society of America*, *347*, pp.1-17.

Gehrels, G., 2011. Detrital zircon U-Pb geochronology: Current methods and new opportunities. *Tectonics of sedimentary basins: Recent advances*, pp.45-62.

Gollan, M., 2006. Plutonic petrogenesis and mineralisation in southwest Fiordland. *Unpublished MSc thesis, University of otago, Dunedin, New Zealand.*

Froude, D.O., Ireland, T.R., Kinny, P.D., Williams, I.S., Compston, W., Williams, I.R. and Myers, J.S., 1983. Ion microprobe identification of 4,100–4,200 Myr-old terrestrial zircons. *Nature*, *304*(5927), pp.616-618.

Ibañez-Mejia, M., Pullen, A., Pepper, M., Urbani, F., Ghoshal, G. and Ibañez-Mejia, J.C., 2018. Use and abuse of detrital zircon U-Pb geochronology—A case from the Río Orinoco delta, eastern Venezuela. *Geology*, *46*(11), pp.1019-1022.s.

Ireland, T.R., Flottmann, T., Fanning, C.M., Gibson, G.M. and Preiss, W.V., 1998. Development of the early Paleozoic Pacific margin of Gondwana from detrital-zircon ages across the Delamerian orogen. *Geology*, *26*(3), pp.243-246.

Kimbrough, D.L., Tulloch, A.J., Coombs, D.S., Landis, C.A., Johnston, M.R. and Mattinson, J.M., 1994. Uranium-lead zircon ages from the median tectonic zone, New Zealand. *New Zealand journal of geology and geophysics*, *37*(4), pp.393-419.

Kimbrough, D.L. and Tulloch, A.J., 1989. Early Cretaceous age of orthogneiss from the Charleston Metamorphic Group, New Zealand. *Earth and planetary science letters*, *95*(1-2), pp.130-140.

Lamb, S. and Mortimer, N., 2021. Taking time to twist a continent—Multistage origin of the New Zealand orocline. *Geology*, *49*(1), pp.56-60.

Leary, R.J., Smith, M.E. and Umhoefer, P., 2020. *Grain-size control on detrital zircon* *cycloprovenance in the late Paleozoic Paradox and Eagle basins, USA. Journal of Geophysical Research: Solid Earth*, 125(7), p.e2019JB019226.

Lovera, O.M., Grove, M., Cina, S. and Kimbrough, D.L., 2008, December. A generalized Kolmogorov-Smirnovstatistic for detrital zircon analysis of modern rivers. In *American Geophysical Union, Fall Meeting 2008,abstract.*

Mapes, R.W., Coleman, D.S., Nogueira, A. and Housh, T., 2004, May. How far do zircons travel? Evaluating the significance of detrital zircon provenance using the modern Amazon River fluvial system. In *Geol. Soc. Am. Abstr. Programs* (Vol. 36, No. 7, p. 78).

Mapes, R.W., Coleman, D.S., Cox, R. and Nogueira, A., 2005, October. Significant changes in the detrital zircon age signature along a transect of the modern Amazon River. In *Geological Society of America Abstracts with Programs* (Vol. 37, No. 4, p. 481)s.

Martin, A.P., Turnbull, R.E., Rattenbury, M.S., Cohen, D.R., Hoogewerff, J., Rogers, K.M., Baisden, W.T. and Christie, A.B., 2016. The regional geochemical baseline soil survey of southern New Zealand: design and initial interpretation. *Journal of Geochemical Exploration*, *167*, pp.70-82.

Mattinson, J.M., 2010. Analysis of the relative decay constants of 235U and 238U by multi-step CA-TIMS measurements of closed-system natural zircon samples. *Chemica Geology*, *275*(3-4), pp.186-198.

McCoy-West, A.J., Mortimer, N. and Ireland, T.R., 2014. U–Pb geochronology of Permian plutonic rocks, Longwood Range, New Zealand: implications for Median Batholith–Brook Street Terrane relations. *New Zealand Journal of Geology and Geophysics*, *57*(1), pp.65-85.

Moecher, D.P. and Samson, S.D., 2006. Differential zircon fertility of source terranes and natural bias in the detrital zircon record: Implications for sedimentary provenance analysis. *Earth and Planetary Science Letters*, *247*(3-4), pp.252-266.

Miller, E.L., Soloviev, A.V., Prokopiev, A.V., Toro, J., Harris, D., Kuzmichev, A.B. and Gehrels, G.E., 2013. Triassic river systems and the paleo-Pacific margin of northwestern Pangea. *Gondwana Research*, *23*(4), pp.1631-1645.

Mortimer, N., 2004. *New Zealand's geological foundations. Gondwana research*, 7(1), pp.261-272.

Mortimer, N., *Arizona Geological Society Digest* 22 2008.

Mortimer, N., van den Bogaard, P., Hoernle, K., Timm, C., Gans, P.B., Werner, R. and Riefstahl, F., 2019. *Late Cretaceous oceanic plate reorganization and the breakup of Zealandia and Gondwana. Gondwana Research*, 65, pp.31-42

Mortimer, N., Hoernle, K., Hauff, F., Palin, J.M., Dunlap, W.J., Werner, R. and Faure, K., 2006. *New constraints on the age and evolution of the Wishbone Ridge, southwest Pacific Cretaceous microplates, and Zealandia–West Antarctica breakup. Geology*, 34(3), pp.185-188.

Mortimer, N., Campbell, H.J., Tulloch, A.J., King, P.R., Stagpoole, V.M., Wood, R.A., Rattenbury, M.S., Sutherland, R., Adams, C.J., Collot, J. and Seton, M., 2017. Zealandia: Earth's hidden continent. *GSA today*, *27*(3), pp.27-35.

Mortimer, N., Rattenbury, M.S., King, P.R., Bland, K.J., Barrell, D.J.A., Bache, F., Begg, J.G., Campbell, H.J., Cox, S.C., Crampton, J.S. and Edbrooke, S.W., 2014. High-level stratigraphic scheme for New Zealand rocks. *New Zealand Journal of Geology and Geophysics*, *57*(4), pp.402-419.

Muir, R.J., Ireland, T.R., Weaver, S.D. and Bradshaw, J.D., 1996. Ion microprobe dating of Paleozoic granitoids: Devonian magmatism in New Zealand and correlations with Australia and Antarctica. *Chemical geology*, *127*(1-3), pp.191-210.

Muir, R.J., Ireland, T.R., Weaver, S.D., Bradshaw, J.D., Evans, J.A., Eby, G.N. and Shelley, D., 1998. Geochronology and geochemistry of a Mesozoic magmatic arc system, Fiordland, New Zealand. *Journal of the Geological Society*, *155*(6), pp.1037-1053.

Nadin, E., Goddard, S., Benowitz, J. and O'Sullivan, P., 2022. Blowing in the late Cenozoic wind—detrital zircon river contributions to an interior Alaska loess deposit. *Quaternary Science Reviews*, *275*, p.107266

Nemchin, A.A., Giannini, L.M., Bodorkos, S. and Oliver, N.H.S., 2001. *Ostwald ripening as a possible mechanism for zircon overgrowth formation during anatexis: theoretical constraints, a numerical model, and its application to pelitic migmatites of the Tickalara Metamorphics, northwestern Australia. Geochimica et Cosmochimica Acta*, 65(16), pp.2771-2788.

O'Sullivan, G.J., Chew, D.M. and Samson, S.D., 2016. *Detecting magma-poor orogens in the detrital record*. *Geology*, *44*(10), pp.871-874.

Press William H., Flannery, Brian P., Teukolsky, Saul A., and Vetterling, William T., 2002.

Numerical Recipes: The Art of Scientific Computing, 2nd Ed., Cambridge University Press, pp. 997.

Press, W.H., Teukolsky, S.A., Vetterling, W.T., and Flannery, B.P., 2007, *Numerical Recipes: TheArt of Scientific Computing (third edition): New York, Cambridge University Press*, 1256 p.

Price, R.C., Ireland, T.R., Maas, R. and Arculus, R.J., 2006. SHRIMP ion probe zircon geochronology and Sr and Nd isotope geochemistry for southern Longwood Range and Bluff Peninsula intrusive rocks of Southland, New Zealand. *New Zealand Journal of Geology and Geophysics*, *49*(3), pp.291-303.

Ringwood, M.F., Schwartz, J.J., Turnbull, R.E. and Tulloch, A.J., 2021. Phanerozoic record of mantle-dominated arc magmatic surges in the Zealandia Cordillera. *Geology*, *49*(10), pp.1230-1234.

Rubatto, D., Williams, I.S. and Buick, I.S., 2001. *Zircon and monazite response to prograde metamorphism in the Reynolds Range, central Australia. Contributions to Mineralogy and Petrology*, 140(4), pp.458-468.

Satkoski, A.M., Wilkinson, B.H., Hietpas, J. and Samson, S.D., 2013. Likeness among detrital zircon populations—An approach to the comparison of age frequency data in time and space. *Bulletin*, *125*(11-12), pp.1783-1799.

Saylor, J.E., Knowles, J.N., Horton, B.K., Nie, J. and Mora, A., 2013. *Mixing of source populations recorded in detrital zircon U-Pb age spectra of modern river sands. The Journal of Geology*, 121(1), pp.17-33.

Saylor, J.E. and Sundell, K.E., 2016. *Quantifying comparison of large detrital geochronology data sets. Geosphere*, 12(1), pp.203-220.

Schwartz, J.J., Klepeis, K.A., Sadorski, J.F., Stowell, H.H., Tulloch, A.J. and Coble, M.A., 2017. *The tempo of continental arc construction in the Mesozoic Median Batholith, Fiordland, New Zealand*. *Lithosphere*, *9*(3), pp.343-365.

Schwartz, J.J., Stowell, H.H., Klepeis, K.A., Tulloch, A.J., Kylander-Clark, A.R., Hacker, B.R. and Coble, M.A.,2016. *Thermochronology of extensional orogenic collapse in the deep crust ofZealandia. Geosphere*, 12(3), pp.647-677.

Scott, J.M. and Palin, J.M., 2008. LA-ICP-MS U-Pb zircon ages from Mesozoic plutonic rocks in eastern Fiordland, New Zealand. *New Zealand Journal of Geology and*

Geophysics, *51*(2), pp.105-113.

Thomas, W.A., 2011. Detrital-zircon geochronology and sedimentary provenance. *Lithosphere*, *3*(4), pp.304-308.

Tulloch, A.J., Ireland, T.R., Kimbrough, D.L., Griffin, W.L. and Ramezani, J., 2011. Autochthonous inheritance of zircon through Cretaceous partial melting of Carboniferous plutons: the Arthur River Complex, Fiordland, New Zealand. *Contributions to Mineralogy and Petrology*, *161*(3), pp.401-421.

Timm, C., Hoernle, K., Werner, R., Hauff, F., van den Bogaard, P., White, J., Mortimer, N. and Garbe-Schönberg, D., 2010. *Temporal and geochemical evolution of the Cenozoic intraplate volcanism of Zealandia. Earth-Science Reviews*, 98(1-2), pp.38-64.

Tulloch, A.J., Kimbrough, D.L., Faure, K., Allibone, A.H., Blevin, P.L., Jones, M. and Chappell, B.W., 2003, July. Paleozoic plutonism in the New Zealand sector of Gondwana. In *Ishihara Symposium, Macquarie University, July 2003.*

Tulloch, A.J., Kimbrough, D.L., Landis, C.A., Mortimer, N. and Johnston, M.R., 1999. Relationships between the Brook Street terrane and Median Tectonic Zone (Median batholith): evidence from Jurassicconglomerates. *New Zealand Journal of Geology and Geophysics*, *42*(2), pp.279-293.

Tulloch, A.J., Ramezani, J., Mortimer, N., Mortensen, J., van den Bogaard, P. and Maas, R., 2009. Cretaceous felsicvolcanism in New Zealand and Lord Howe Rise (Zealandia) as a precursor to final Gondwana break-up. *Geological Society, London, Special Publications*, *321*(1), pp.89-118.

Turnbull, I.M. and Allibone, A.H., 2003. *Geology of the Murihiku area. Institute of Geological & Nuclear Sciences.*

Turnbull, R.E., Tulloch, A.J. and Ramezani, J., 2013. Zetland Diorite, Karamea Batholith, west Nelson: field relationships, geochemistry and geochronology demonstrate links to the Carboniferous Tobin Suite. *New Zealand Journal of Geology and Geophysics*, *56*(2), pp.83-99.

Turnbull, R., Weaver, S., Tulloch, A., Cole, J., Handler, M. and Ireland, T., 2010. Field and geochemical constraints on mafic–felsic interactions, and processes in high-level arc magma chambers: an example from the Halfmoon Pluton, New Zealand. *Journal of Petrology*, *51*(7), pp.1477-1505.

Waight, T.E., Weaver, S.D., Ireland, T.R., Maas, R., Muir, R.J. and Shelley, D., 1997. Field characteristics, petrography, and geochronology of the Hohonu Batholith and the adjacent Granite Hill complex, NorthWestland, New Zealand. *New Zealand Journal of Geology and Geophysics*, *40*(1), pp.1-17.

Walcott, R.I., 1978. Present tectonics and late Cenozoic evolution of New Zealand. *Geophysical Journal International*, *52*(1), pp.137-164.

Williams, I.S., 2001. *Response of detrital zircon and monazite, and their U–Pb isotopic systems, to regional metamorphism and host-rock partial melting, Cooma Complex, southeastern Australia. Australian Journal of Earth Sciences*, 48(4), pp.557-580.

Van der Meer DG, Van Hinsbergen DJ, Spakman W. Atlas of the underworld: Slab remnants in the mantle, their sinking history, and a new outlook on lower mantle viscosity. Tectonophysics. 2018 Jan 16;723:309-448.

Vermeesch, P., 2018. IsoplotR: *A free and open toolbox for geochronology. Geoscience Frontiers*, 9(5), pp.1479-1493.

Vita

Will Sparhawk Fisher was born in Albany NY, September 9th 1997. They attended Union College and received an honors B.S. degree in Geology in 2019. The following fall they enrolled in Earth Science Department at Syracuse University, to pursue a M.S. in Earth Science. They now work at Los Alamos National Laboratory as a Nuclear Forensic Investigator employing actinide geochemistry and radiochemistry.